A STUDY OF PROTEINASES OF INVASIVE CELLS USING CRYOULTRAMICROTOMY AND IMMUNOGOLD LABELLING

Edith Elliott
M.Sc. (Natal)

Submitted in fulfilment of the
academic requirements for the degree
of
Doctor of Philosophy
in the
Department of Biochemistry
University of Natal

Pietermaritzburg

1993

VOLUME TWO

PLATES

PLATE 1

Overview of cryoultramicrotomy sections of density gradient separated polymorphonuclear leucocyte fractions.

Figure 1. Leucocyte cell types seen in a typical Ficoll-Hypaque density gradient PMN fraction.

PMNs (P) show evidence of osmotic distress, manifest as degranulation (arrowheads). Activation is also evident in PMNs (AP = activated PMN) and monocytes (M) as shown by the presence of some macrophages (Ma). "PMN fractions" are also contaminated with lymphocytes (L), thrombocytes (t) and dendritic cells (DC).

Figure 2. Leucocyte cell types seen in a typical Percoll density gradient PMN fraction.

PMNs (P) show less evidence of osmotic distress, or evidence of degranulation. No evidence of PMN (P) or monocyte (M) activation is evident. "PMN fractions" are contaminated with fewer lymphocytes, but still contain thrombocytes (t) and dendritic cells (DC). Erythrocytes (R) also contaminate preparations.
PS = "band" or "stab" (immature) form of PMN.

Figure 3. A dendritic cell.

Dendritic cells are characterised by an irregular outline, with moderately smooth surface lamellipodia, eccentric, elongated, lobulated nucleus (Nu), and a nucleus/cytoplasm ratio of 1:2. The cytoplasm contains some vacuoles and appears generally less dense, with granules of a different morphology compared to macrophages and monocytes.

Figure 4. A dendritic cell.

The cell shown manifests blunt pseudopodia of varying length, an eccentric, elongated, lobulated nucleus, with many indentations and euchromatic karyoplasm with condensation at the outer edge of the nuclei. The cytoplasm and granules are comparable to those of the cell shown in Fig. 3.

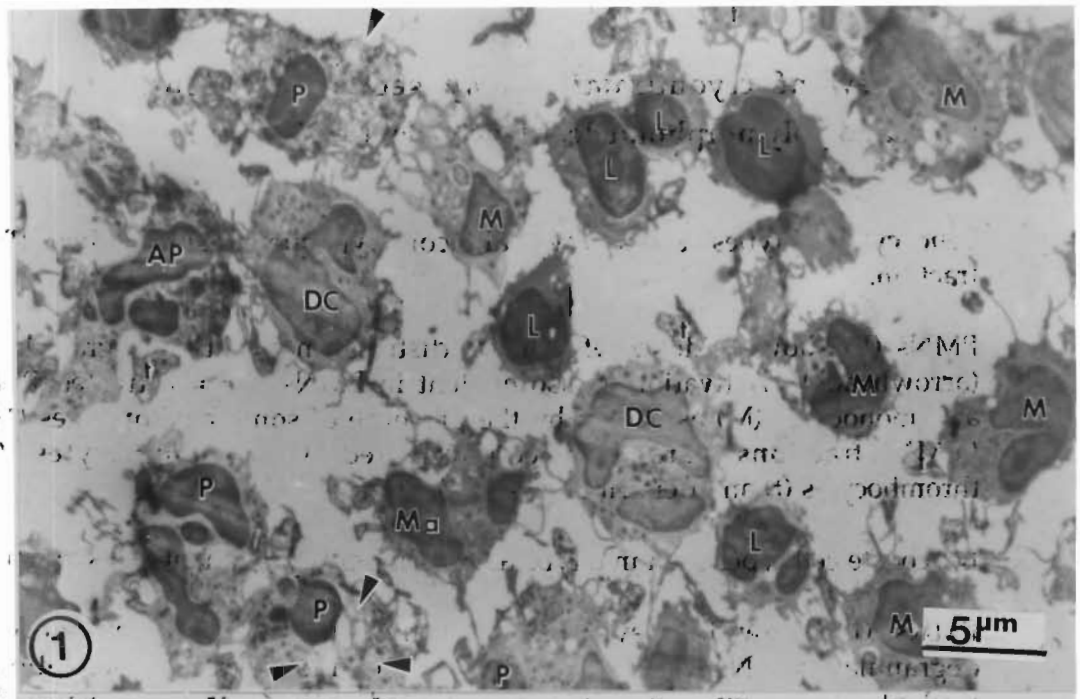
P
M
L
AP
DC
M
P
P
5µm
1

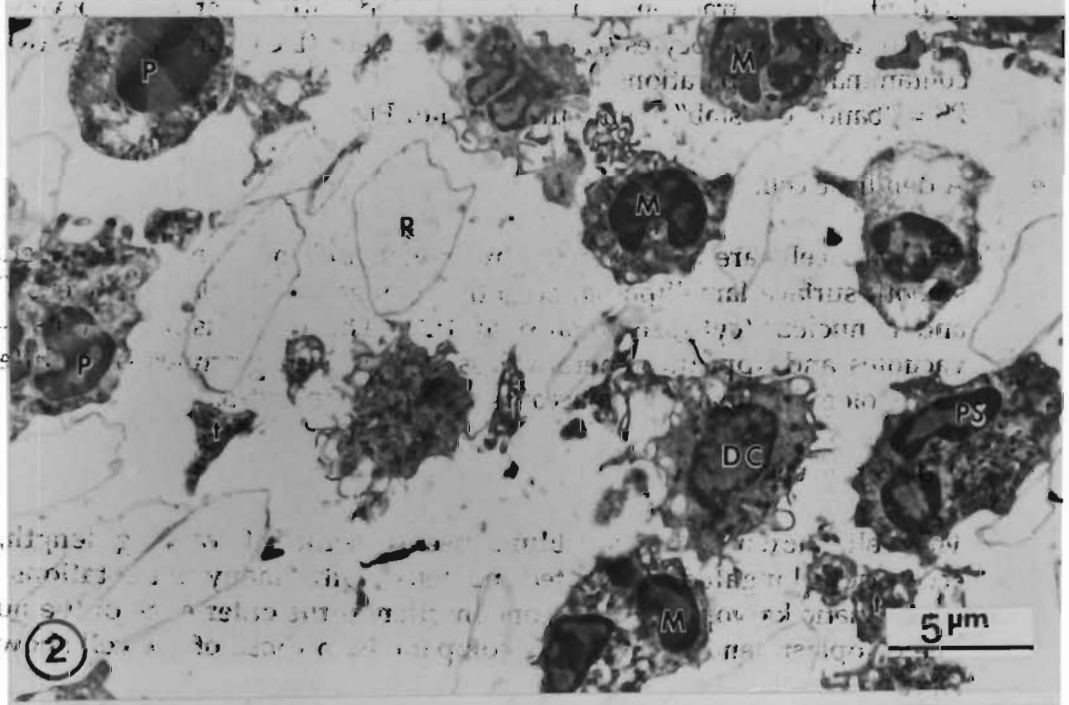
P
M
R
M
P
DC
PS
M
5µm
2

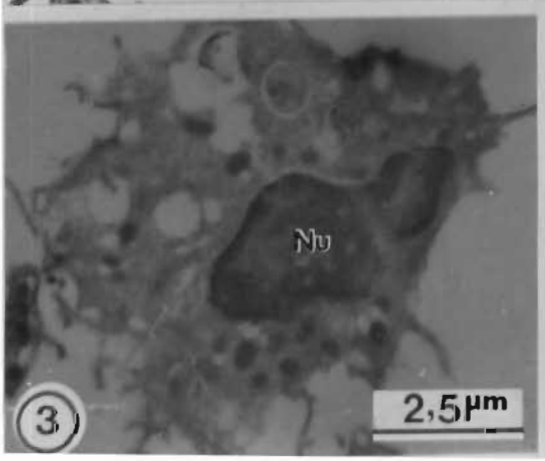
Nu
2,5µm
3

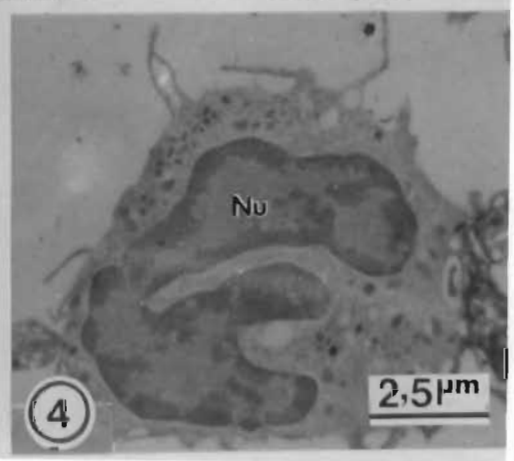
Nu
2,5µm
4

PLATE 2

Unembedded cryoultramicrotomy sections of PMNs (and other cells), variously fixed with PFA and labelled for elastase.

Figure 1. A non-activated PMN fixed with 8% PFA, pH 7.2.

Fixation was in HEPES buffer (15 min) and labelling for elastase, **without flotation** on fixative prior to immunolabelling and **without post-labelling fixation.** Note failure of preservation of cytoplasmic integrity and almost complete extraction of azurophil granules.

Figure 2. Non-activated PMN fixed with 4% PFA, pH 7.2, and 8% PFA, pH 7.2.

Fixation was in HEPES buffer (15 min) and labelling for elastase, **without flotation** on fixative prior to immunolabelling for elastase, and **with post-labelling** fixation (with 1% glutaraldehyde). Note extremely poor ultrastructure and poor antigen immobilisation.

Figure 3. Leucocyte fraction fixed with 4% PFA, pH 7.2 and 8% PFA, pH 7.2.

Sections were fixed for 5 and 10 min, respectively, **floated** on 8% PFA, pH 7.2, (30-60 min) prior to labelling, and **post-fixed** with 1% glutaraldehyde, all in HEPES buffer.

a Different mononuclear cells and a PMN. Note good ultrastructural preservation.

b A non-activated PMN - labelling for elastase detected with a 10 nm gold probe. Note improved ultrastructure compared to Figs 1 and 2, but remaining translation of elastase antigen (arrows).

Figure 4. A non-activated PMN, fixed in 4% and 8% PFA, at pH 7.2, in cacodylate buffer.

Fixation was for 5 min and 1 h, respectively, and a peroxidase reaction product was generated, to assist the stabilisation of azurophil granules (arrows, and see also inset), sections labelled for elastase with **no flotation**, but **post-labelling fixation** (with 1% glutaraldehyde). Note success of such stabilisation but failure of elastase immobilisation.

Figure 5. PMA activated PMN fixed with 8% PFA, pH 8.0.

Fixation (in HEPES buffer, 15 min). The section was **not floated** on fixative before labelling, but was **fixed** with glutaraldehyde, **post-labelling** for elastase. Note immobilisation of elastase antigen, but apparent poor maintenance of azurophil granule integrity (swollen appearance subsequently found to be the result of cell activation).

Bar scale on all micrographs = 1 μm (inset bar = 0.5 μm).

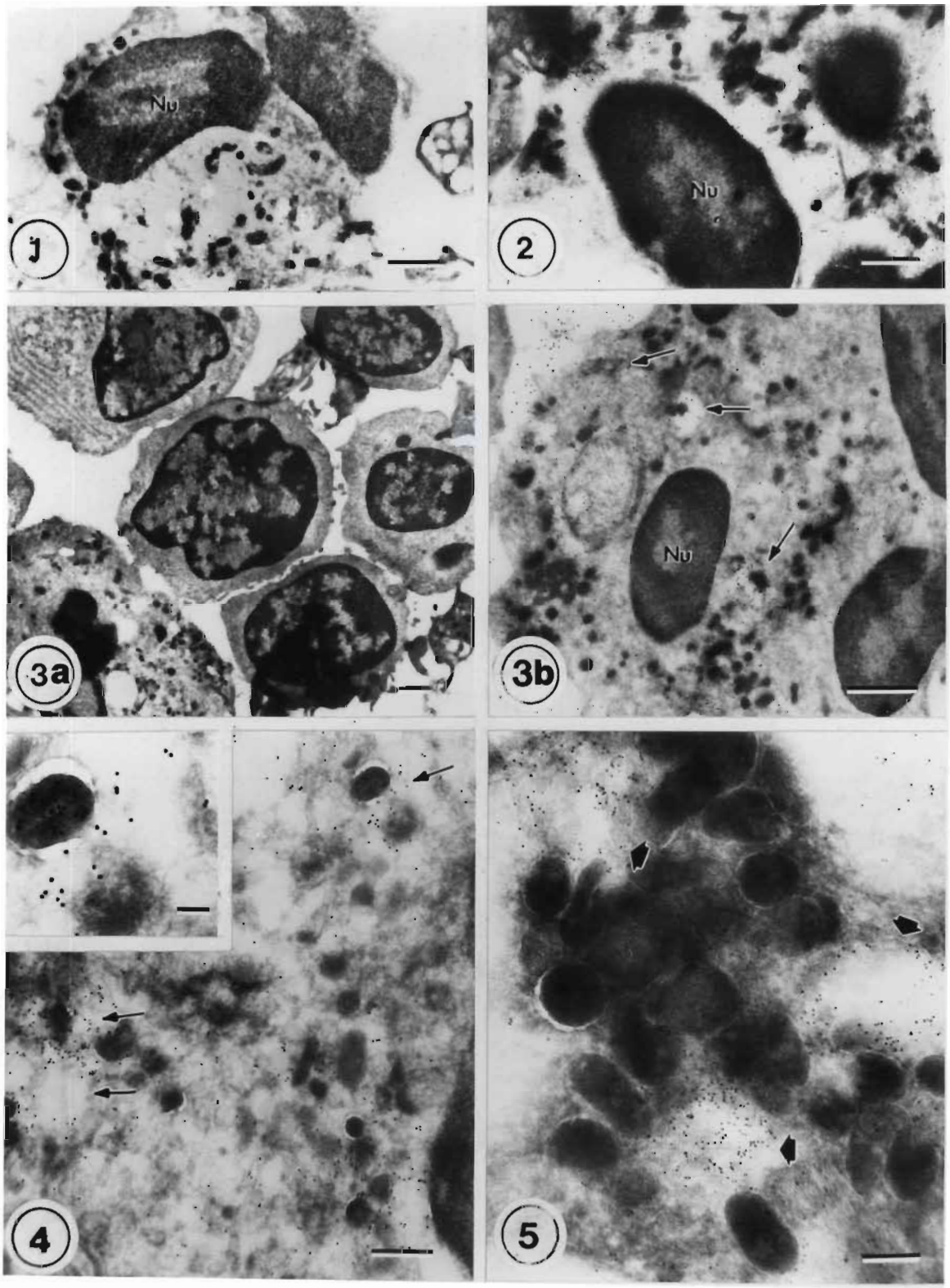
Nu
1
Nu
2
3a
Nu
3b
4
5

PLATE 3

Non-activated PMNs fixed with 4% PFA, pH 8.0 and 8% PFA, pH 7.2, in HEPES buffer, with and without flotation prior to labelling, but with post-labelling fixation.

Figure A. Non activated PMNs labelled for elastase and myeloperoxidase.

PMNs fixed with 4% PFA, pH 8.0 (5 min), followed by 8% PFA, pH 7.2 (10 min), in HEPES buffer. Sections were **not floated** on fixative prior to labelling, but were **fixed, post-labelling** for elastase or myeloperoxidase (inset), with 1% glutaraldehyde.
Overview of cell shows slight translation of the antigen, and azurophil granule contents appears "shrunken" (arrows).
Inset shows similar extraction of the azurophil antigen, myeloperoxidase.

Figure B. Non-activated PMN labelled for cathepsin D and lactoferrin.

Cells were fixed and **not floated** on fixative prior to labelling, as for **A**. Labelling for cathepsin D (5 nm) and lactoferrin (10 nm) was performed with a protein A-gold probe, and **fixed post-labelling** with 1% glutaraldehyde.
Partial extraction of large granules (possibly azurophil granules) labelled for cathepsin D is evident (large arrow), whereas smaller granules, also labelled for cathepsin D, which are not specific granules (as they are labelled for lactoferrin, small arrows), remain largely unextracted. Translation of these antigens does not seem to occur.

Figure C. Non activated PMN, labelled for elastase and lactoferrin (inset).

Cells were fixed and **floated** on fixative prior to labelling. Labelling was for elastase, and sections were **fixed post-labelling** with 1% glutaraldehyde.

Note swelling of azurophil granules, thought to be caused by initial high pH fixation and possibly exaggerated, either by **flotation** on pH 8.0 fixative, prior to immunolabelling, or by marginal cell activation during density gradient isolation. Adequate containment of elastase is achieved by this approach. Note the suggestion of a "tubular" body (arrowhead) which would possibly be seen more clearly in "thick" sections (see Section 4.5.1). Morphology of specific granules is unaffected by the fixation procedure.
Inset shows labelling of specific granules for lactoferrin.

Bar scale on inset = 10 μm, on other micrographs = 1 μm

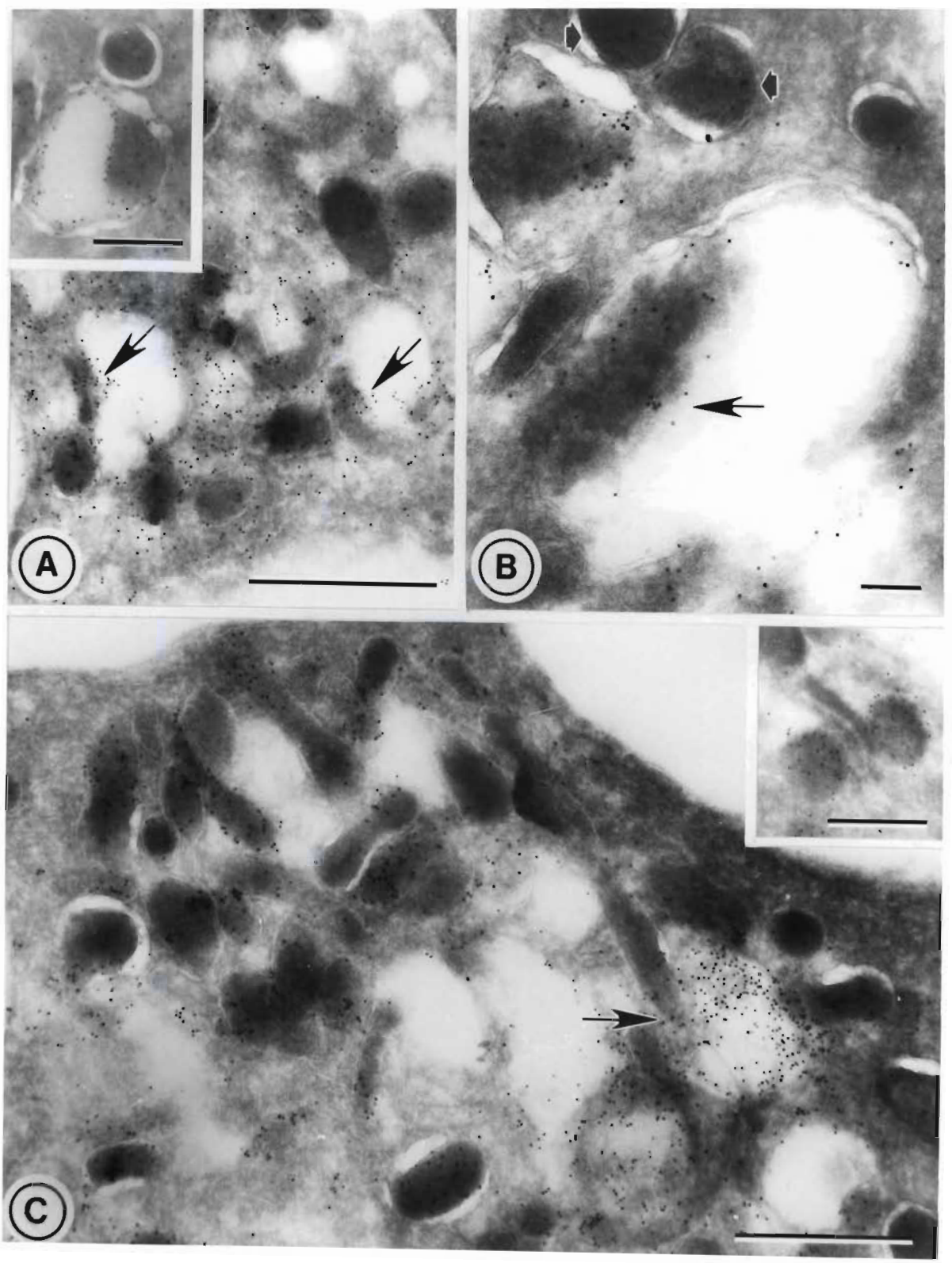
A
B
C

PLATE 4

Immunofluorescence labelling demonstration of the surface distribution of elastase (and cathepsin G) in PMNs activated by PMA and fMLP.

Figure 1. Labelling of unpermeabilised fMLP-activated PMN cells.

Percoll density gradient separated PMNs (2.4×10^6) activated *in vitro* with fMLP (30 μM, 30-45 min, 37°C), spread on a slide and immediately fixed and labelled for elastase, show a polarised surface distribution of elastase, consistent with the association of elastase with the "leading edge" of the chemotactically activated cells. Labelling for cathepsin G (not shown) is similar.
Note that eosinophils show the most intense immunolabelling.

Figure 2. Labelling of unpermeabilised PMA-activated PMN cells.

PMNs, prepared as described in Fig. 1, activated with PMA (40 μM, 30-45 min, 37°C) and labelled for elastase, show a general, non-polarised, distribution of elastase. Labelling for cathepsin G (not shown) gave similar results.

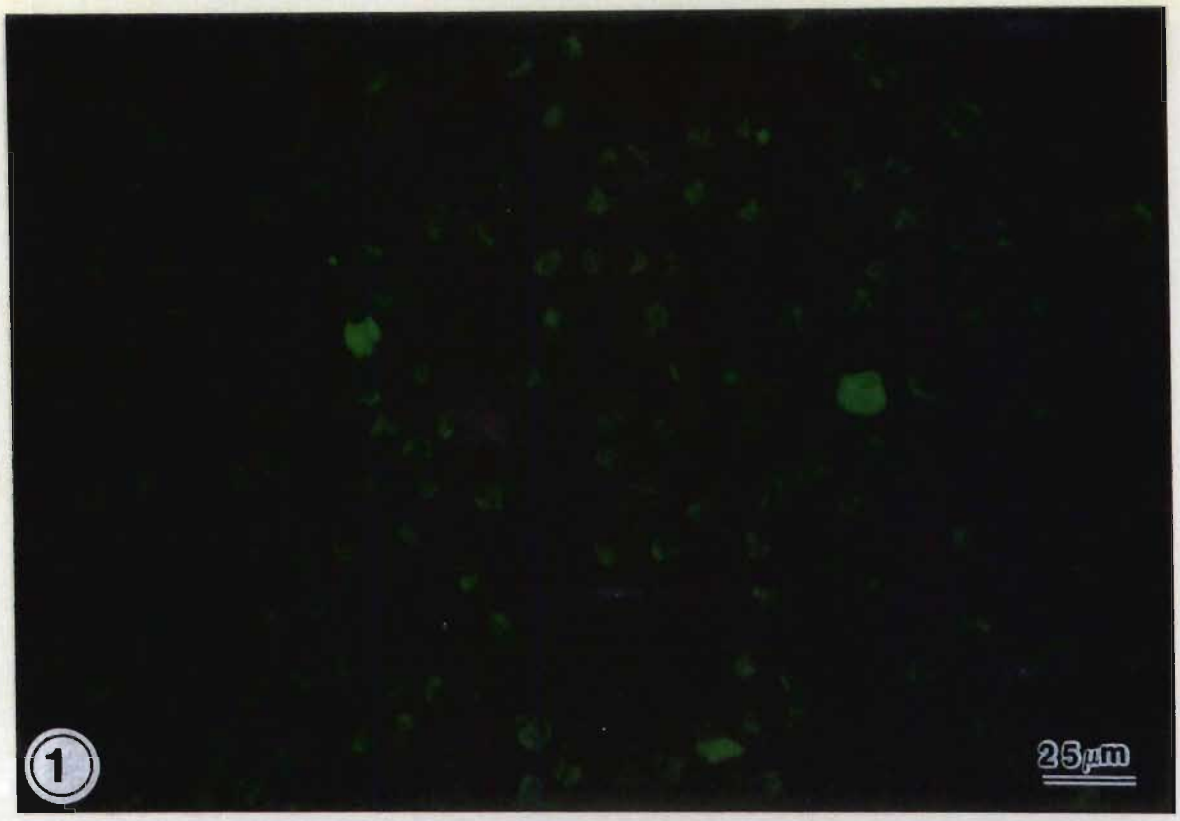
1
25μm

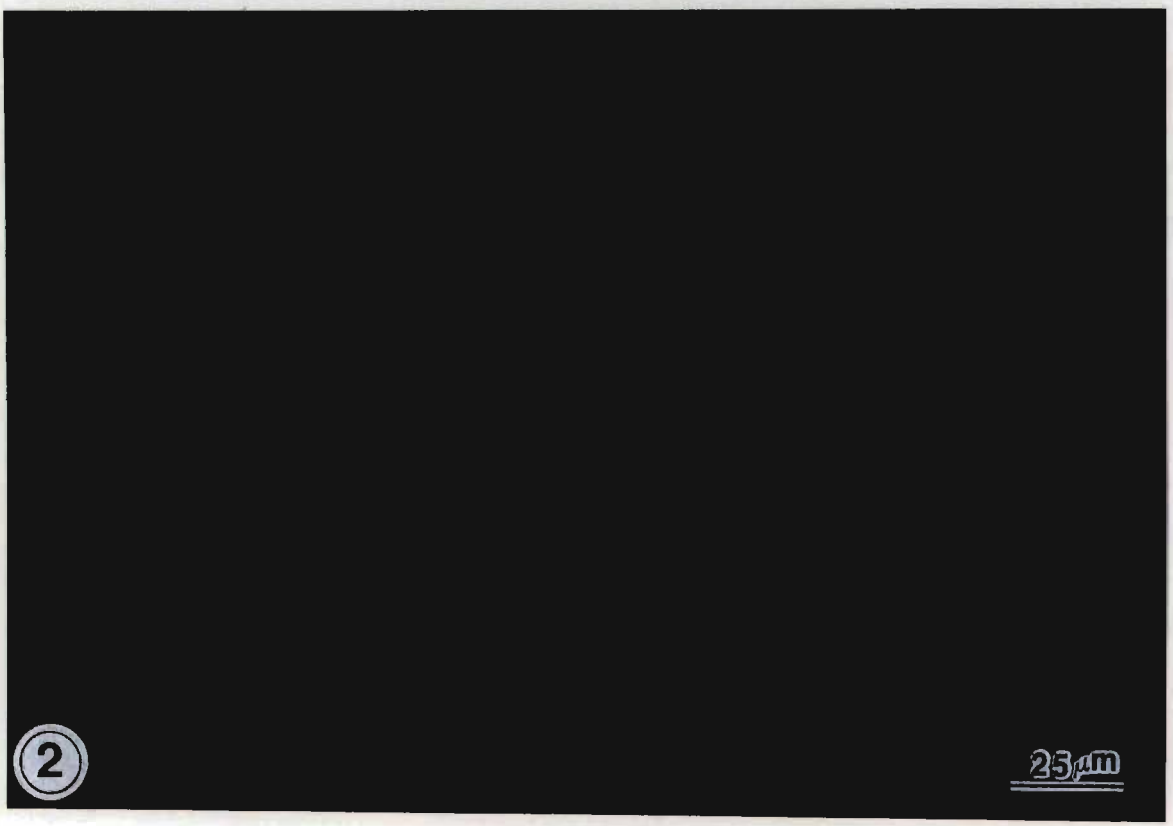
2
25μm

PLATE 5

"Cryo" study of the effects of fMLP activation on the PMN cell function and distribution of elastase.

Figure 1. Morphological evidence of effects of fMLP-activation on cell function and surface distribution of elastase.

Percoll density gradient separated PMNs (2.4×10^6) activated *in vitro* with fMLP (30 μM, 30-45 min, 37°C), fixed with 8% PFA, pH 8.0 (5 min) followed by 8% PFA, pH 7.2 in HEPES buffer (15 min), were processed for cryoultramicrotomy, and labelled for elastase.

The shape of the cell indicates motion in the direction in which the granules are polarised within the cell. Labelling shows association of elastase with the electron-dense, intact surface or "leading edge" of the cell (large arrows mid cell) and with the the diffuse ruffled surface of the upper part of the cell (large arrows, upper part of cell). Less surface associated elastase occurs on the opposite side of the cell away from the leading edge (arrowheads) but no elastase is associated with the "trailing edge" (see Fig. 2). A few electron-translucent granules containing elastase are visible, but none of the large electron-translucent compartments that are obvious in the body of PMA-activated PMNs (see especially Plate 6). Small arrows indicate some degranulation, but no pinocytic- or phagocytic activity is evident. Labelling for cathepsin G shows similar results (Not shown). Nu= nucleus

Figure 2. Overview of fMLP-activated PMN showing trailing edge.

Trailing edge of the fMLP-activated cell is indicated by large arrows, the ruffled surface being indicated by arrowheads.

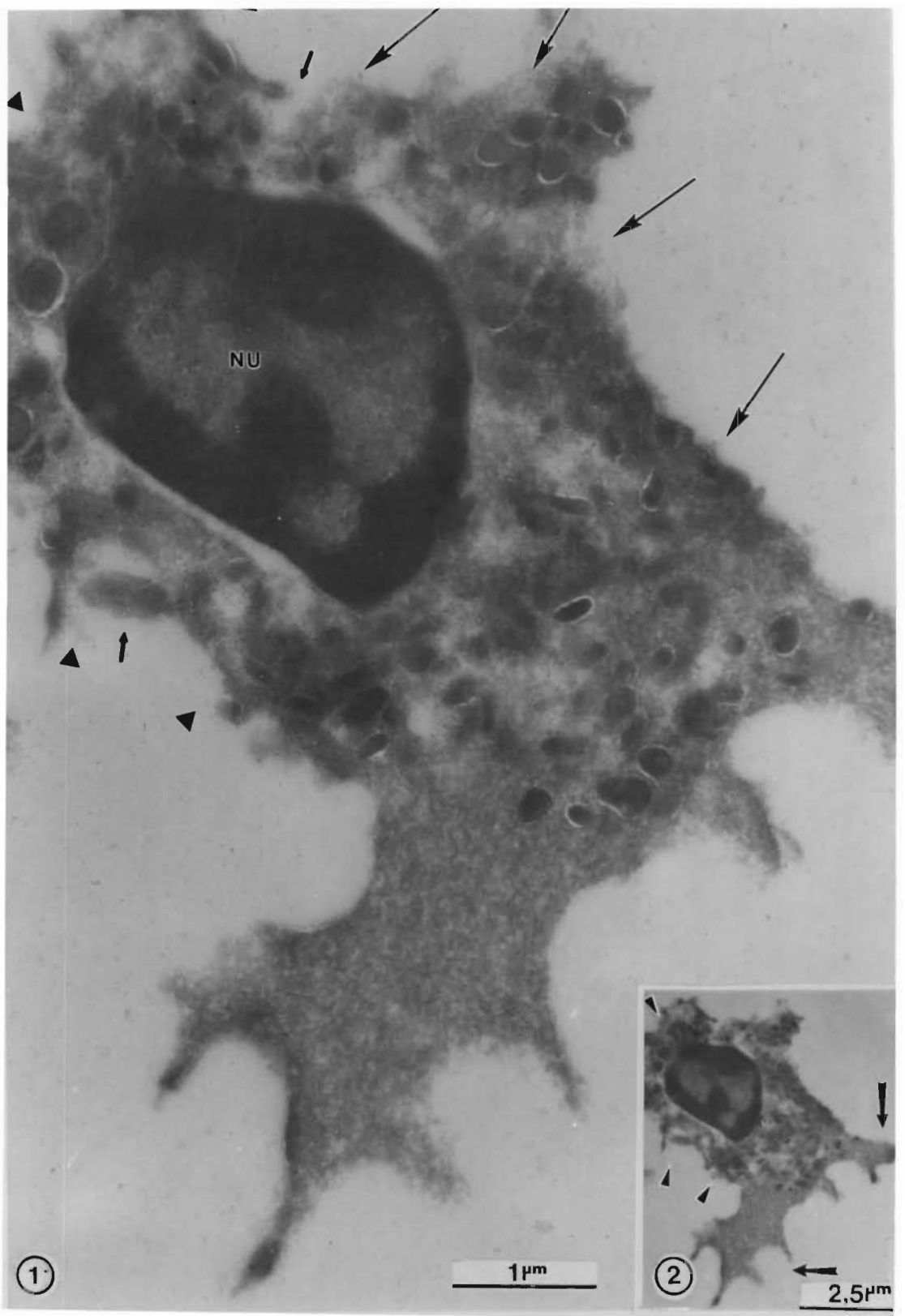
NU
1
1µm
2
2,5µm

PLATE 6

"Cryo" study of the effects of low levels of PMA (25 μM) activation on cell function and distribution of elastase, in activated PMNs.

Figure 1. Effects of low level PMA-activation on cell morphology, function and surface distribution of elastase.

Cells isolated and activated with PMA (25 μM) (30-45 min, 37°C), fixed and prepared as described previously (PLATE 5, Fig 1), were labelled for elastase.

Stimulation with low levels of PMA gives rise to increased pinocytosis (P = pinocytotic or phagocytic vesicles), some polarisation of granules towards one side of the cell, similar to that seen in chemotactic activation, ("leading edge" indicated with large thin arrows) and the development of a "trailing edge" (large short fat arrows). Some elastase does become associated with the surface of the cell (short thin arrow), but far less than in fMLP activated cells (PLATE 5, Fig. 1). Unique large electron-translucent elastase (and cathepsin G-)-containing compartments, possibly vestiges of large three-dimensional tubular compartments are evident (see discussion Section 4.5.1.4). Similar results are seen in labelling for cathepsin G (Not shown).

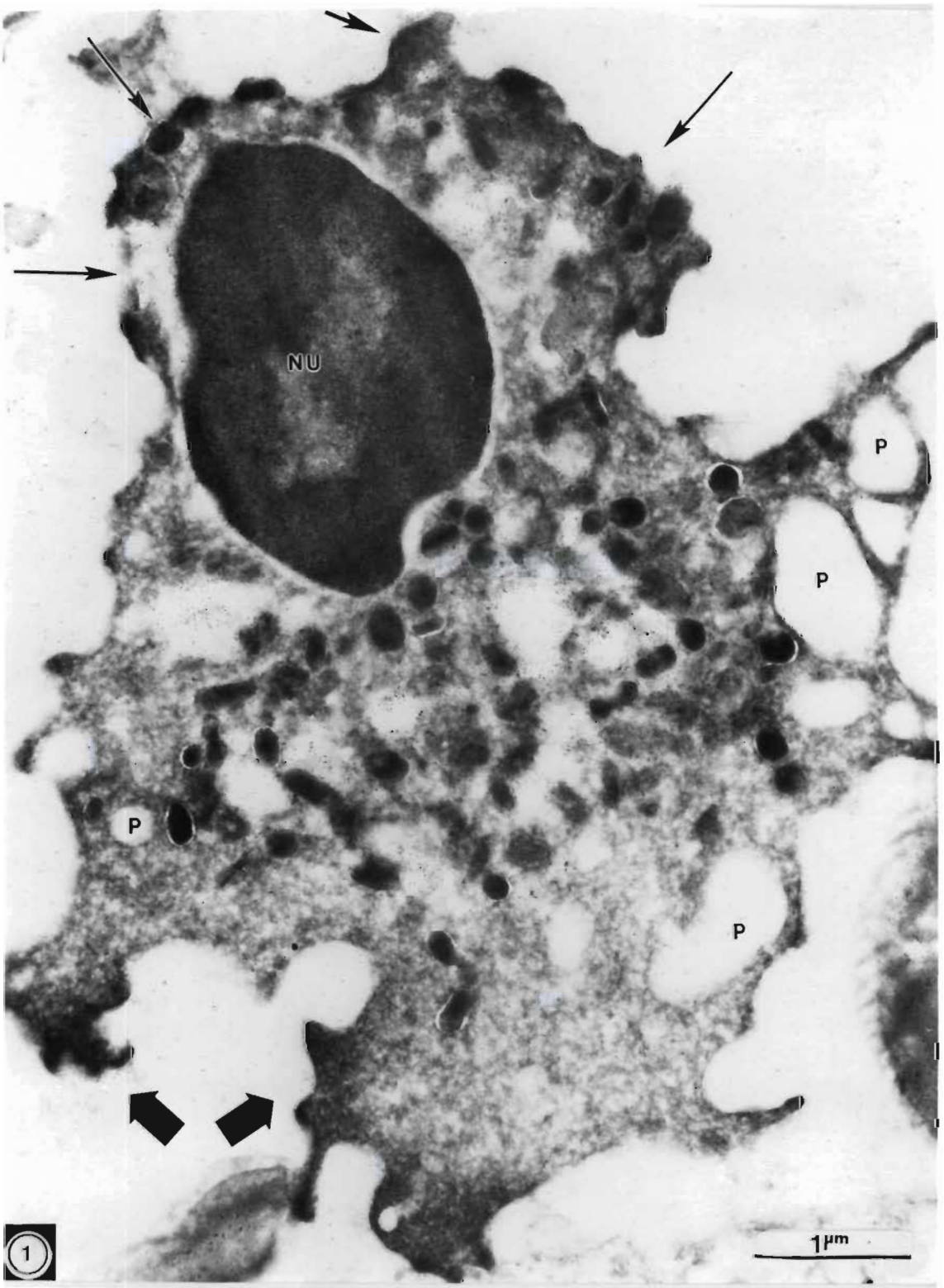
NU
P
P
P
P
1
1μm

PLATE 7

"Cryo" study of the effects of high levels of PMA activation on cell morphology, function and distribution of elastase, in PMNs.

Figs 1-4. Various views of the same PMN cell, labelled for cathepsin G indicating mechanisms whereby the enzyme is released or becomes associated with the surface of the cell. PMNs were isolated and activated with PMA (40 µM, 30-45 min, 37°C), fixed, and prepared for labelling as described previously (PLATE 5, Fig 1). Similar results (not shown) were obtained for elastase.

Figure 1. Cathepsin G release by a degranulation mechanism.

Some degranulation is seen to occur by a process whereby an entire granule is lost, or the contents of a swollen elastase/cathepsin G-containing organelle are expelled (large arrow).

Figure 2. Overall morphology of PMNs activated with 40 µM PMA.

High level PMA stimulation of PMNs results in a rounded morphology, indicative of loss of "movement" related activities including phagocytosis and possibly pinocytosis. Degranulation and release of enzymes often occurs from one side of the cell only (arrows indicate degranulation site shown in Fig. 1). This cell illustrates two mechanisms whereby cathepsin G (and elastase) may become integrated into the cell wall, via a mechanism of exocytosis (Fig. 4) or by association with a diffuse outer cell wall (Fig. 3).

Figure 3. Diffuse cell membrane facilitating association of enzymes.

The opposite side of the cell to that where degranulation is seen to occur (Fig. 2) has a diffuse membrane with which enzymes become associated (cathepsin G indicated by 5 nm protein A gold particles, arrows)

Figure 4. Exocytosis by "integration" of the granules into the cell surface.

Illustration of two granules (black and open arrowheads) in the final stages of integration into the external membrane of the activated PMN. This leads to the formation of a "cup-like" structure with which proteinases seem to be associated, possibly transiently.

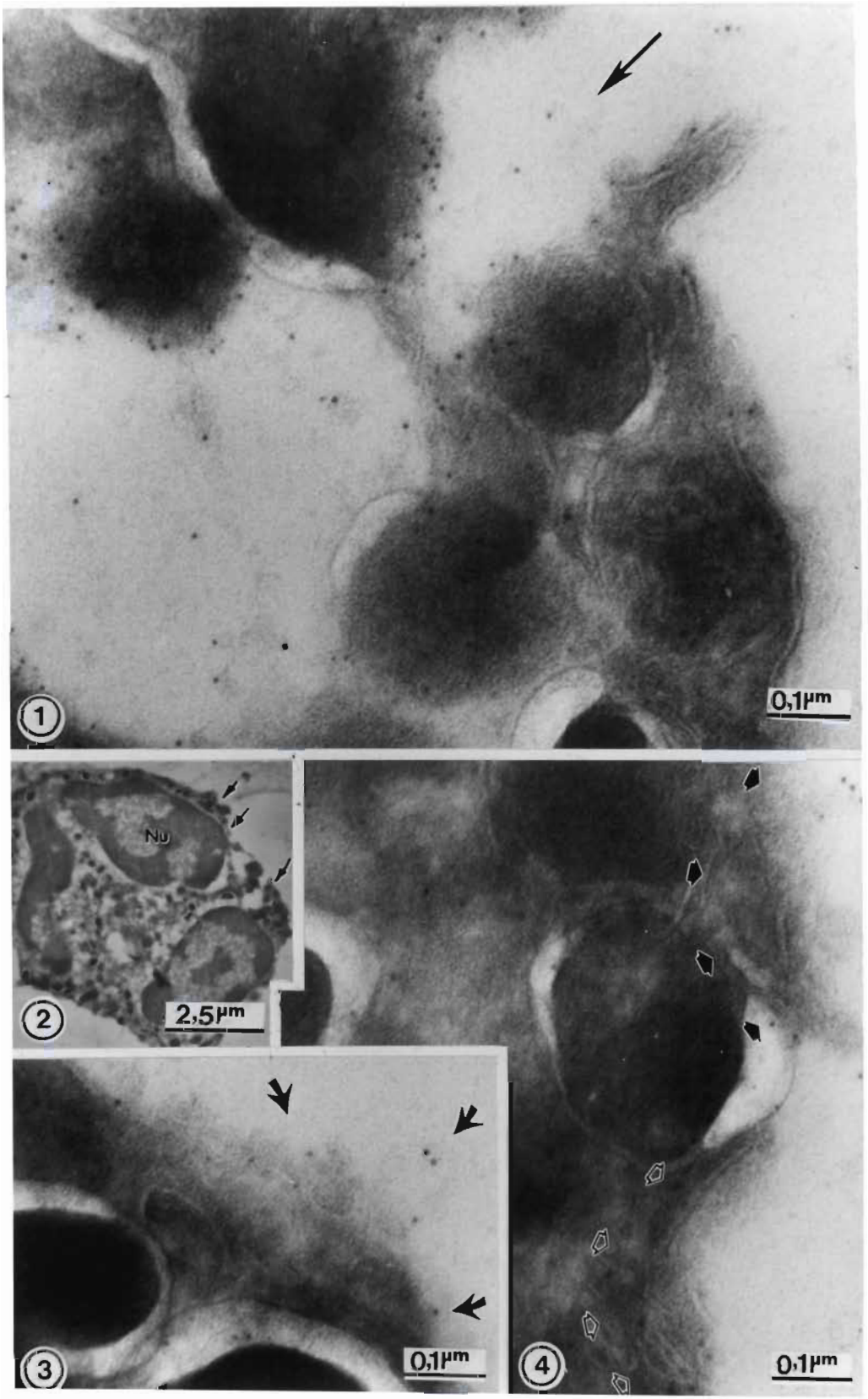
1
0,1µm
Nu
2
2,5µm
3
0,1µm
4
0,1µm

PLATE 8

"Cryo" section of the red pulp region of a human spleen.

Figure 1. Section cut along the axis of a splenic sinus, showing function of endothelial stave cell.

Three endothelial stave cells (E) are seen to form a sinus containing a monocyte (M, lower right hand side plate). Their basal surface is indicated by a semi-continuous basement membrane (small arrows centre micrograph, and arrow far right-hand side). Numerous pinocytotic vesicles are evident on the apical surface of these cells (see just right of lower central arrows). Evidence of phagocytic activity is seen in the central endothelial cell, which contains a platelet (Pl) or thrombocyte. On the left-hand side of this sinus is a cordal space (c) containing two PMNs (P) and an erythrocyte (R) and a resident macrophage (M upper left hand corner). Arrows upper and lower left-hand side of micrograph indicate reticulin fibres of the cordal spaces.

Figure 2. A cross-section of a sinus indicating the positioning of endothelial stave cells.

Endothelial cells line the sinus, their nuclei abutting into the sinus at irregular intervals along the sinus space. A continuous basement membrane (arrows) is seen here, holding these cells together, but this is usually non-continuous at intervals, allowing cells to squeeze through during passage into the cordal spaces (c). R = red cell/erythrocyte.

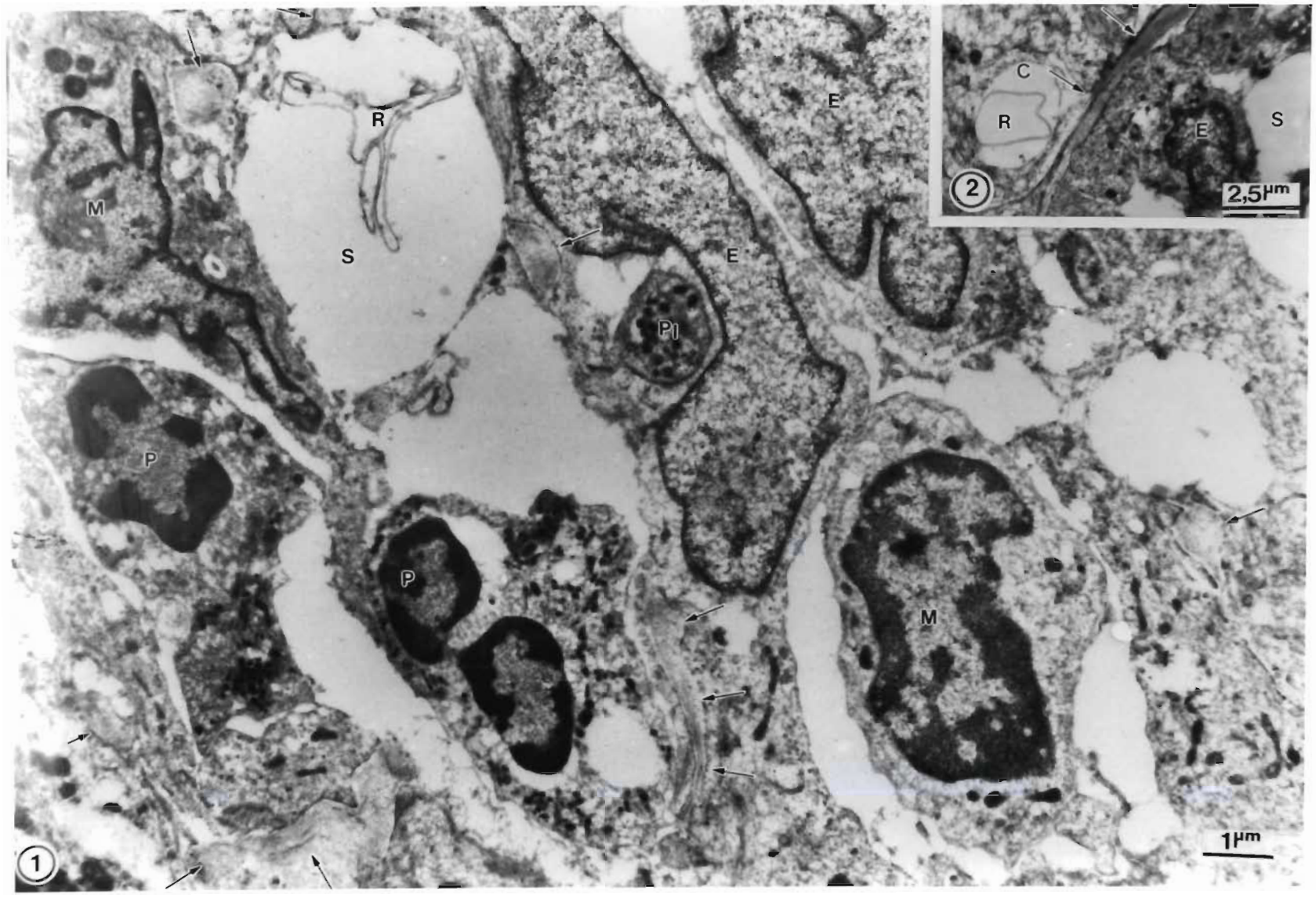
R
E
M
S
E
Pl
P
P
M
1µm
C
R
E
S
2
2,5µm
1

PLATE 9

"Cryo" labelling evidence of possible secondary function of endothelial stave cells.

Figure 1. Evidence of pinocytotic removal of elastase from the splenic sinuses by endothelial stave cells.

An endothelial stave cell (boundary indicated by large arrowheads) showing numerous pinocytotic vesicles (small arrows) filled with elastase (HLE) (5 nm gold particle) and some cathepsin D (12 nm gold particles). Such uptake of HLE was only observed in the presence of activated PMNs. Double labelling indicates the *in vivo* association of elastase (5 nm gold particle, arrowheads) and cathepsin D (10 nm, intermediate sized arrow) with the surface of activated PMNs confirming *in vitro* studies. Colocalisation of labelling for cathepsin D and elastase (an azurophil granule marker enzyme) in some organelles (intermediate sized arrows), but not all granules, supports the hypothesis that azurophil granules are heterogeneous in their enzyme content. A lysosome in the endothelial stave cell is indicated by labelling for cathepsin D (large arrow).

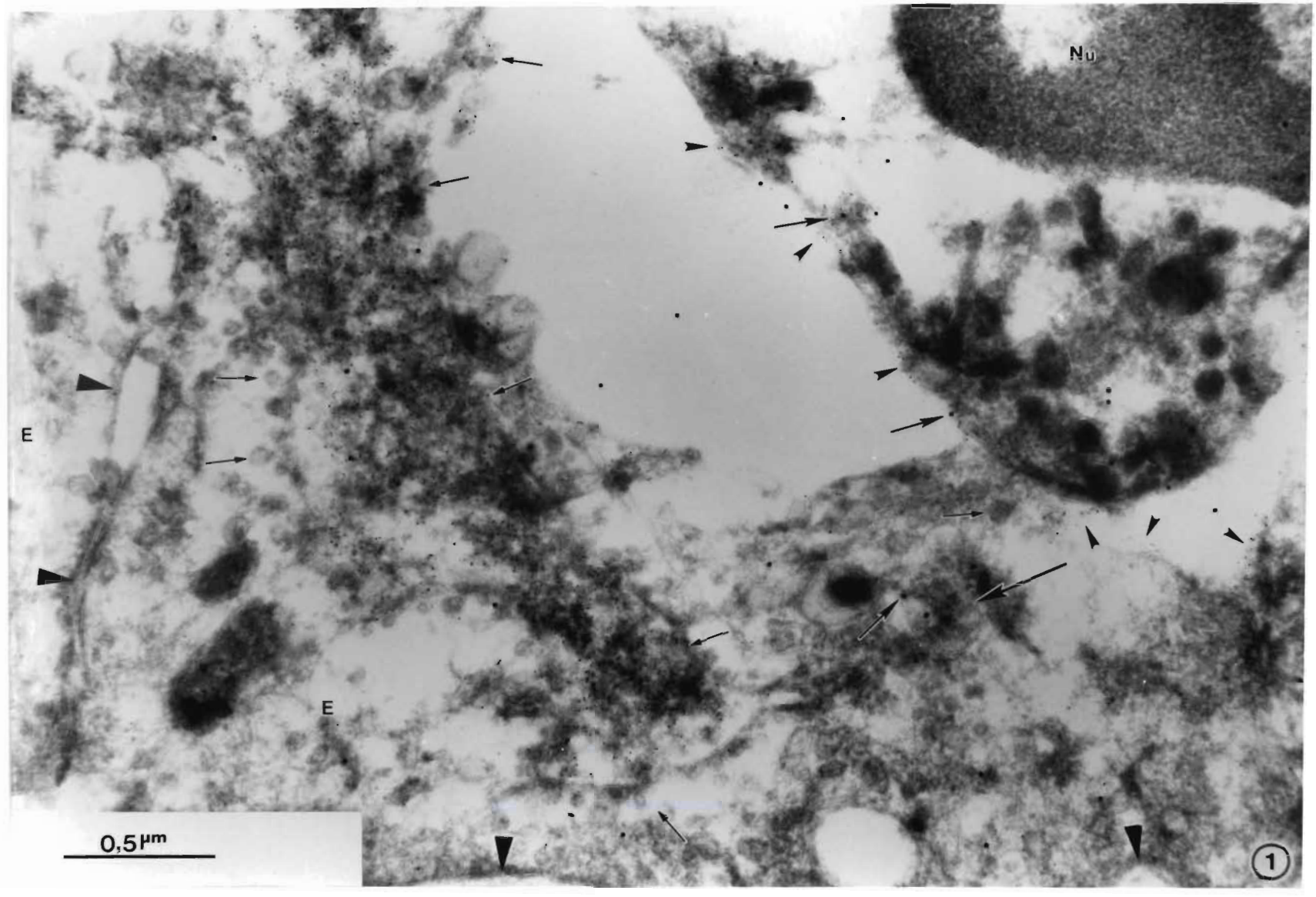
Nu
E
E
0,5 µm
1

PLATE 10

"Cryo" immunolabelling of peripheral blood monocytes and macrophages for elastase.

Figs 1→4. Different magnifications of a monocyte and a macrophage; all sections fixed with 4% PFA, pH 7.2 (5 min) followed by 8% PFA, pH 7.2 (15 min) and labelled for elastase.

Figure 1. Human peripheral blood monocyte.

Arrowheads indicate the presence of elastase, which, may be endogenous (see electron-dense granules labelled for elastase, upper right of micrograph), or endocytosed (large electron translucent pinosome containing elastase – arrowheads, centre of micrograph), and small pinocytotic vesicles on cell surface. No surface labelling for elastase was observed.

Figure 2. Overview of morphology of a peripheral blood monocyte.

Low magnification view shows approx. 1:1 nuclear to cytoplasmic ratio and pinocytotic activity characteristic of monocytes.

Figure 3. Overview of morphology of a peripheral blood macrophage.

Macrophages have a larger cytoplasm to nucleus ratio, greater phagocytic activity (see large amount of cell debris in the largest phagosome, lower arrowhead), and a greater number of granules than in a monocyte (compare Figs 1 and 2).

Figure 4. Higher magnification of peripheral blood macrophage.

Phagosomes and electron-dense organelles (possible lysosomes) are seen to contain elastase (arrowheads). No surface labelling for elastase is visible. Endoplasmic reticulum and mitochondria are not well preserved by the fixation regime used (Section 4.6.1.1).

Nu = nucleus.

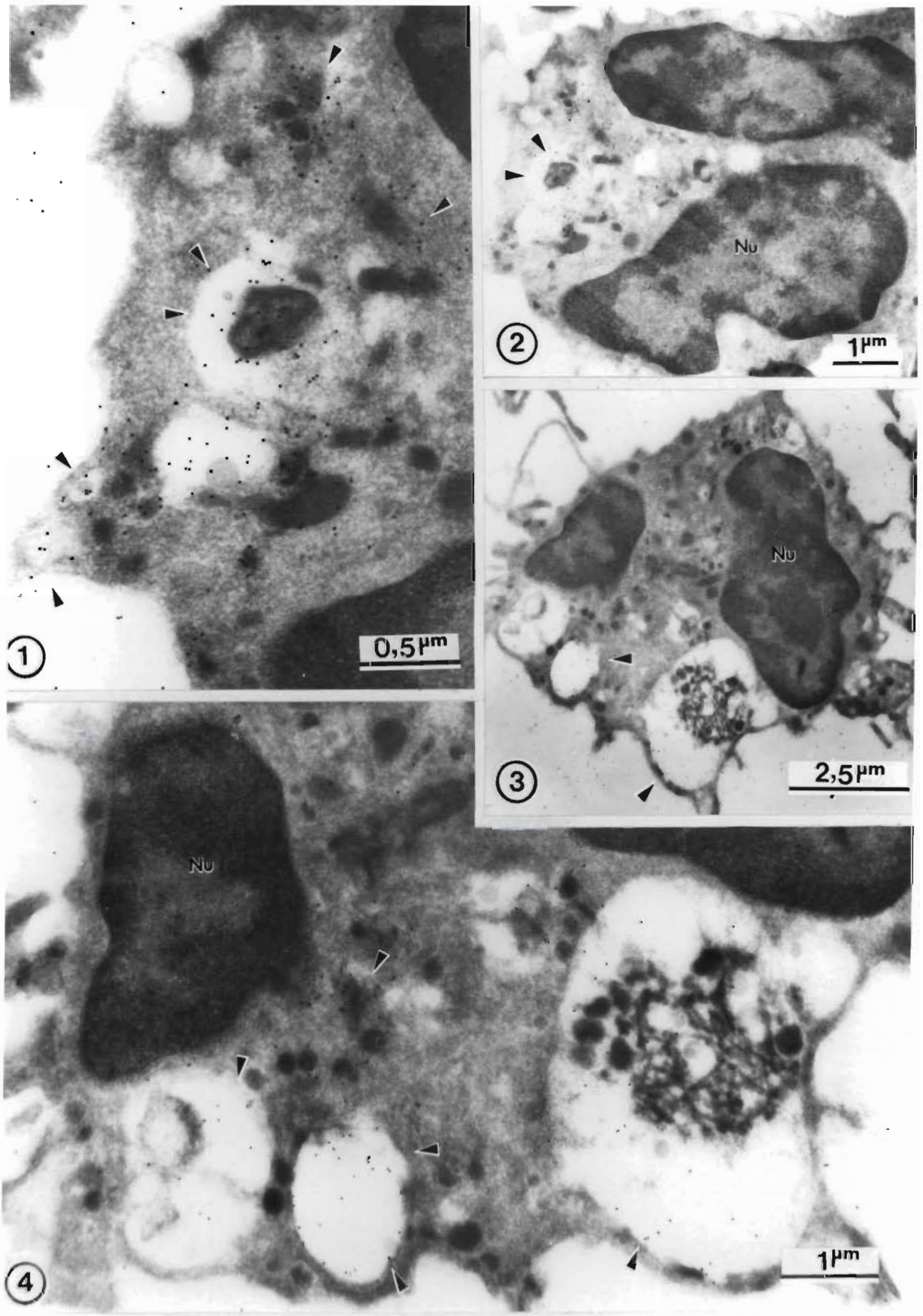
1
0,5µm
2
Nu
1µm
3
Nu
2,5µm
4
Nu
1µm

Plate 11

"Cryo" sections of a plasma cell and endothelial stave cell, of human spleen labelled for cathepsin D and elastase, and cathepsin B and its precursor, respectively

Figs 1→4. Splenic tissue fixed with 8% PFA, pH 8.0 (15 min, RT).

Figs 1 & 2. Plasma cell labelled for cathepsin D and elastase.

Plasma cell showing extensive endoplasmic reticulum (ER) development, numerous mitochondria (M) and immunolabelling for cathepsin D (arrowheads, Fig. 1) and elastase (Fig. 2). Nu = nucleus.

Figs 3 & 4. Double labelling for cathepsin B and procathepsin B on splenic endothelial stave cell. Immunolabelling performed using anti-ppB22-36 antibody (2 μg in 10 μl) and the sheep anti-human liver cathepsin B antibody (0.2 μg in 10 μl), detected with protein A gold labels.

Figure 3. Enlarged view of cathepsin B-containing organelles.

Colocalalization of labelling for procathepsin B (5 nm) and cathepsin B (10 nm) in some electron-dense organelles (arrow and arrowhead), suggest a prelysosomal nature, cleavage of the precursor not yet having occurred. More electron-translucent organelles labelling for mature cathepsin B only (arrowhead only) may be lysosomes.

Figure 4. Overview of endothelial stave cell showing cytoplasmic filaments.

In the basal portion of the endothelial stave cells, electron-dense, filamentous bands (lower right-hand corner) and cytoplasmic filaments (large slender arrow) speculated to confer contractile capabilities on the stave cells are seen. Golgi stacks (G) show labelling with antibodies against precursor (5 nm gold particles) and mature cathepsin B (small arrows), intermediate sized arrow indicates possible prelysosomal compartment and arrowheads, possible lysosome, seen in Fig. 3 above.

M = mitochondrion, Nu = nucleus.

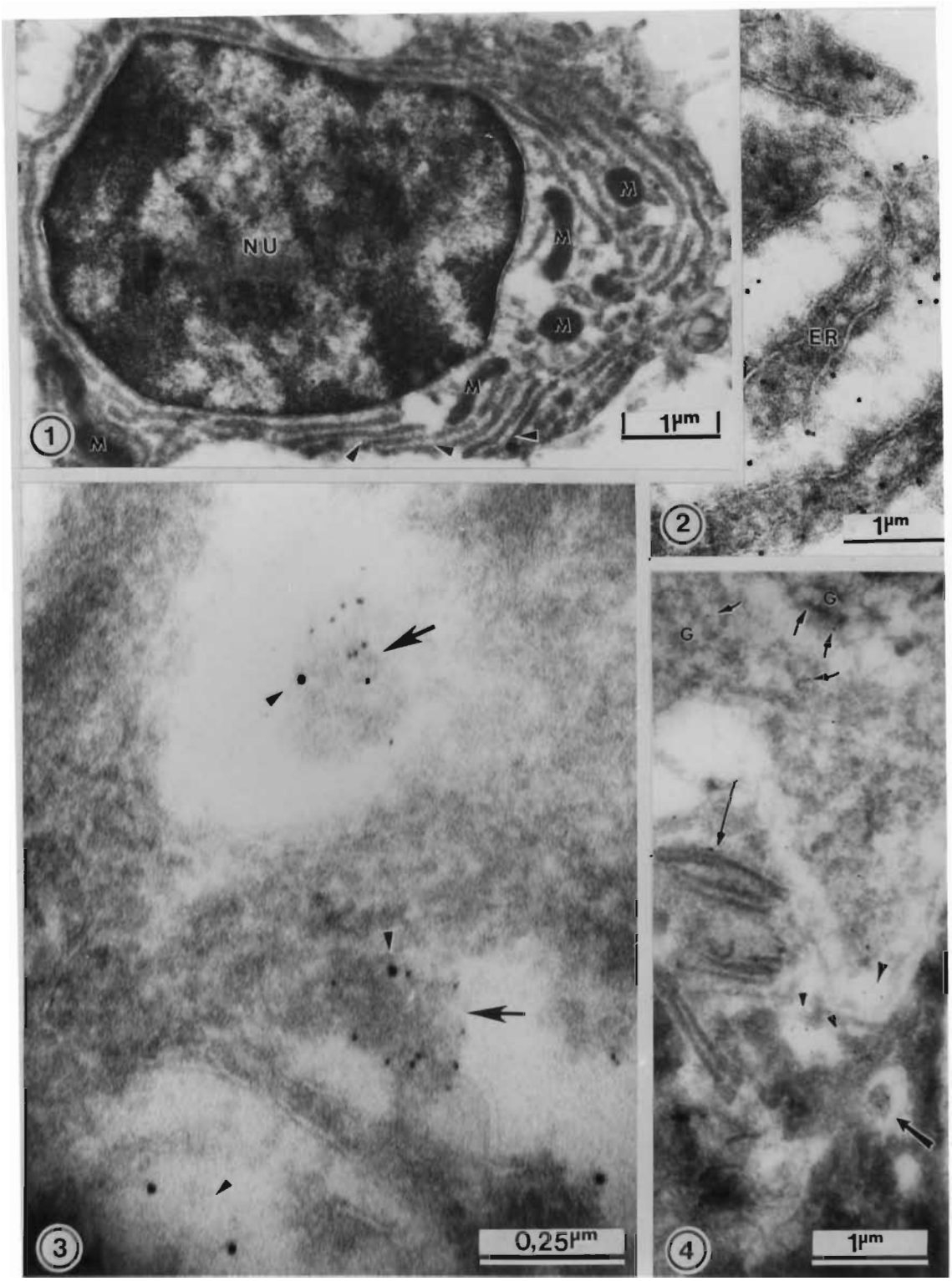
NU
M
M
M
M
M
1
1μm
ER
2
1μm
3
0,25μm
G
G
4
1μm

PLATE 12

LR White embedded sections of human spleen showing splenic macrophage.

Figs 1 & 2. Splenic tissues fixed with 4% PFA containing 0.2% glutaraldehyde in 0.1 M cacodylate buffer, pH 7.2 (15 min, RT).

Figure 1. Macrophage showing secretory vesicles labelling for cathepsin B.

Macrophage showing numerous electron-translucent secretory vesicles (small arrows), larger vesicles showing lower labelling density. Arrowheads indicate cordal reticulin fibre. Notice swelling distortion characteristic of LR White embedded tissue.
Nu = nucleus.

Figure 2 Immunolabelling of immature and mature macrophage secretory granules

Two populations of secretory granules are evident, one labelling for cathepsin B only (small arrows) and some occasional, more electron dense, larger granules label for both cathepsin B and procathepsin B. (small and large arrows).

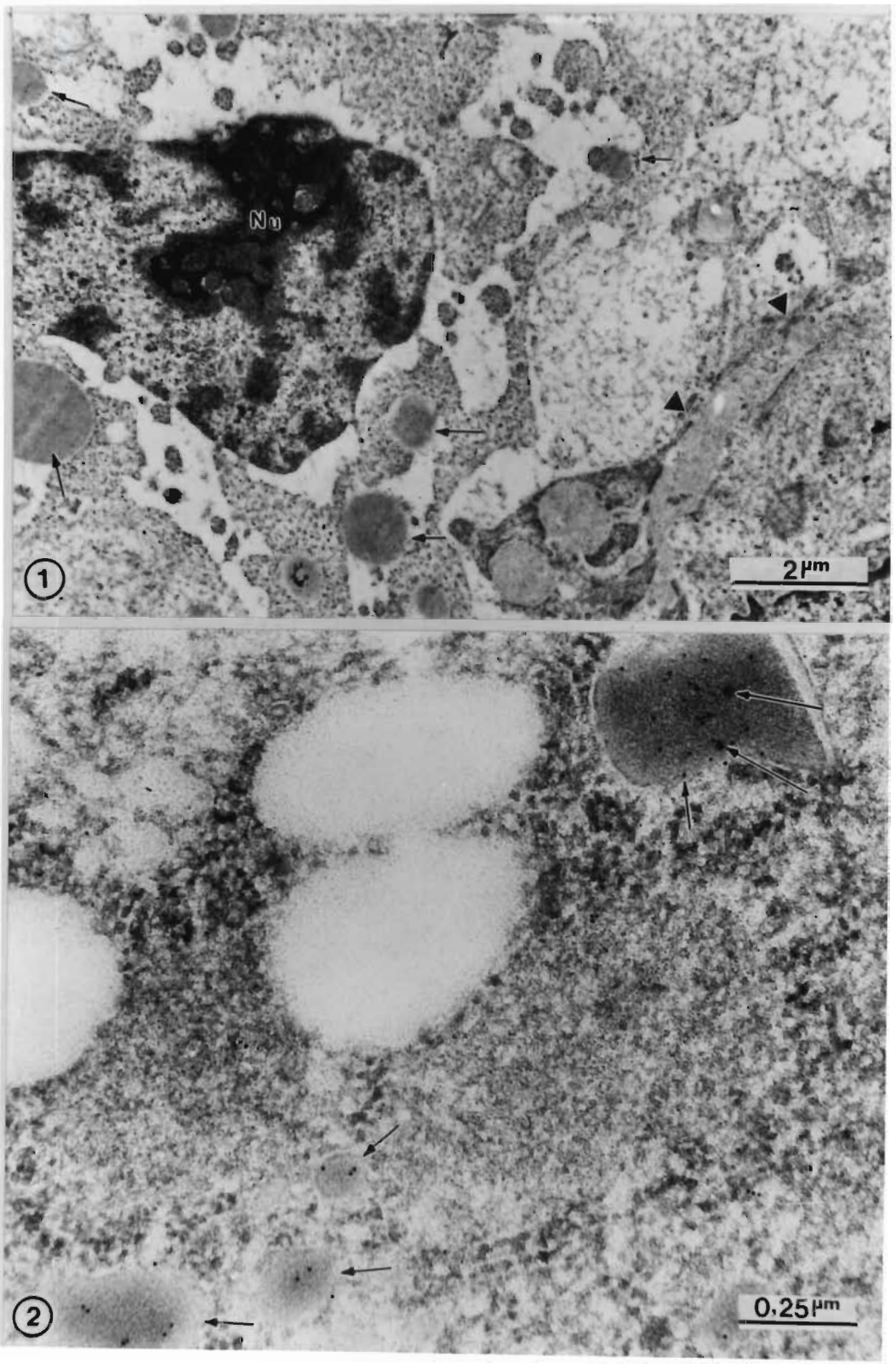
Nn
2μm
0.25μm

PLATE 13

"Cryo" sections of an fMLP-activated macrophage and an unactivated monocyte labelled for procathepsin B or cathepsin D, respectively.

Figs 1→4. Cells fixed with 8% PFA in 200mM HEPES, pH 8.0, 15 min.

Figs 1, 2 & 4. Macrophage activated with fMLP (30 μg/ml), and immunolabelled for procathepsin B with the ppB22-36 antibody (2 μg in 10μl).

Figure 1. Overview of macrophage showing labelling for procathepsin B.

Electron-translucent and some more electron-dense granules show labelling for procathepsin B (small arrows). Note lack of labelling for procathepsin B on cell surface and good preservation/definition of membranes of granules . Nu = Nucleus.

Figure 2. Enlarged view of electron-dense and semi-electron dense granules labelled for procathepsin B.

Note good retention of procathepsin B in electron dense- (lower right) and more electron translucent granules.

Figure 3. Immunolabelling of a monocyte for cathepsin D.

Monocytes contain moderate numbers of vesicles labelled for cathepsin D. (small arrow) and a few mitochondria (M).

Figure 4. fMLP-activated macrophage showing procathepsin B labelling of Golgi stack.

Good membrane preservation due to the use of PFA fixation at pH 8.0 enables the Golgi apparatus (G) to be discerned. As anticipated, this shows labelling for procathepsin B (small arrow). Notice, however, the poor structural preservation of mitochondria (mitochondrion just to the left, above the central electron-dense granule).

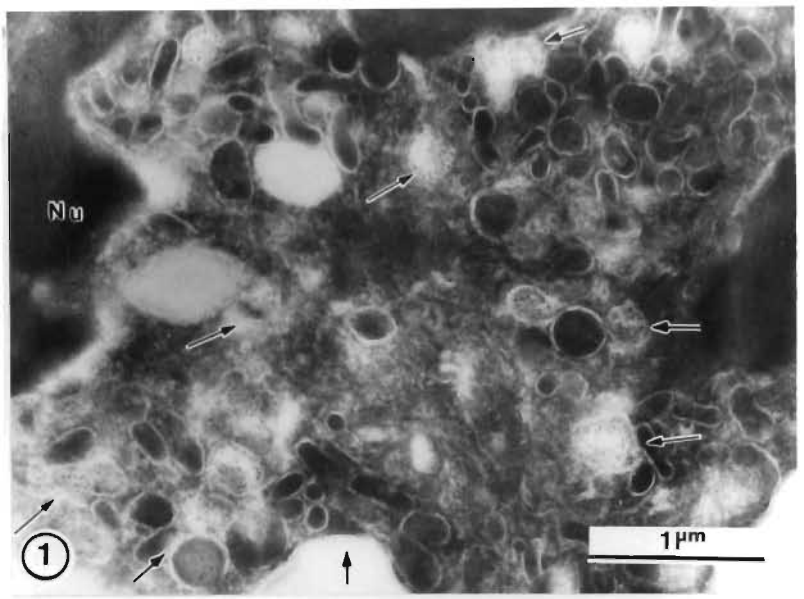

1

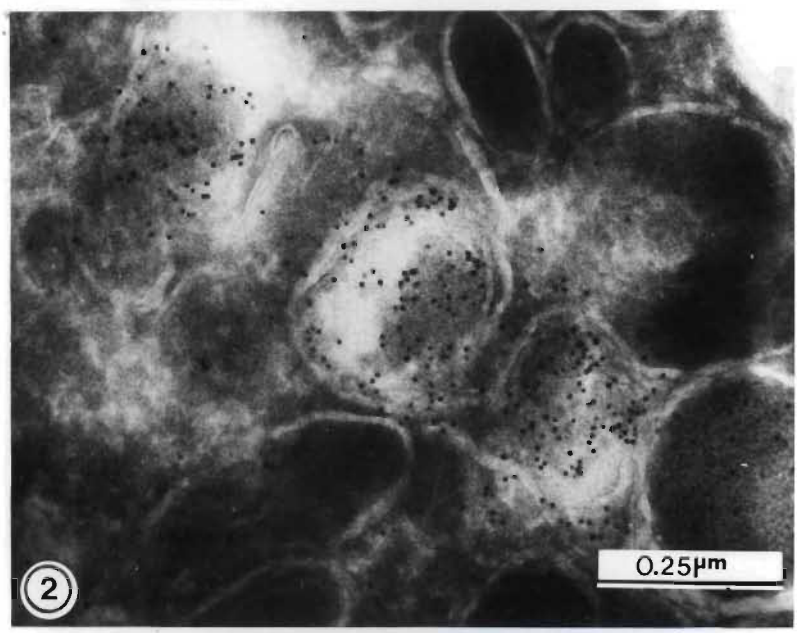

2

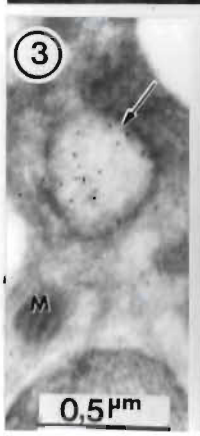

3

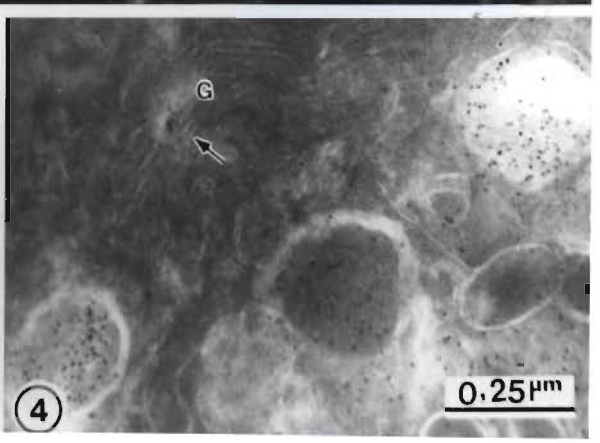

4

PLATE 14

Macrophages labelled for cathepsin B and procathepsin B, showing differences in apparent structural detail due to thickness of the section and the final film of methyl cellulose/uranyl acetate.

Figs 1-3 Macrophages fixed with 8% PFA in 200 mM HEPES, pH 8.0 and immunolabelled with anti-ppB22-36 antibody (2 µg in 10 µl) or sheep anti-human liver cathepsin B antibody (0.2 µg in 10µl), detected with protein A gold label (5 nm).

Figure 1. Macrophage labelled for cathepsin B.

Relatively thick section of a macrophage (120-150 µm) showing labelling for cathepsin B (arrowheads). Membrane preservation is good, but compare with membrane definition of cell in Fig. 2.

Figure 2. Macrophage labelled for procathepsin B.

Moderately thick section of a macrophage (120-150 µm) showing labelling for procathepsin B. Section occurs near a grid bar and, consequently, the final layer of methyl cellulose/uranyl acetate is quite thick. Micrograph, therefore illustrates the improved membrane definition imparted by a thicker final layer of this sealing medium. Micrograph also illustrates how, even in well preserved cryosections, granules may be easily lost. Arrows illustrate extracted granule and hole from which it came, respectively.

Figure 3. Macrophage labelled for cathepsin B.

A relatively thin section (estimated to be 80-100 nm) showing concomitant loss of structural detail of granule morphology. Granules show labelling for cathepsin B (arrowheads). Compare sections shown in Figs 1, 2 and 3.

Nu = nucleus.

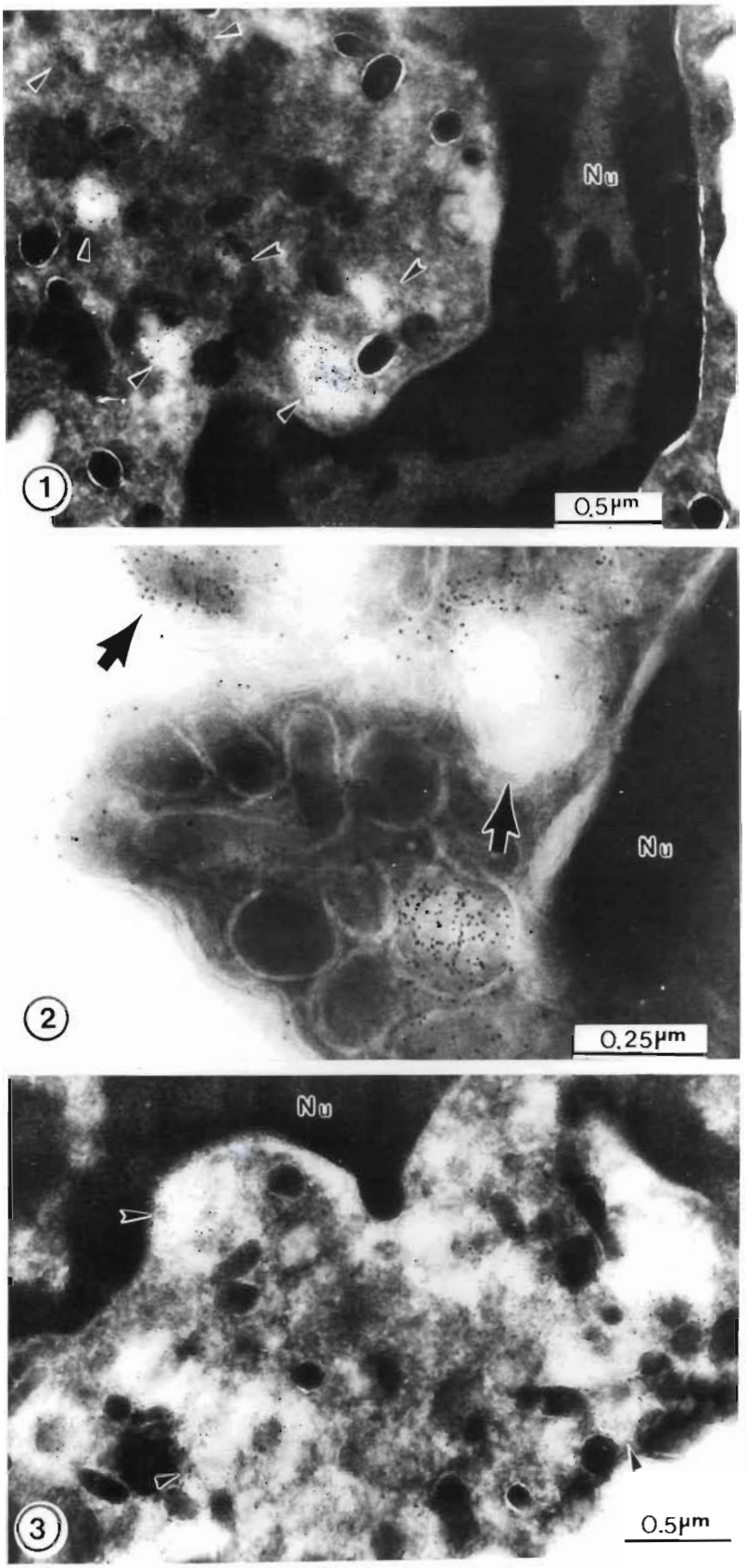
Nu
1
0.5μm
Nu
2
0.25μm
Nu
3
0.5μm

PLATE 15

Fluorescent labelling of permeabilised U937 cells, illustrating cathepsin B, D and elastase labelling seen in undifferentiated- and PMA- and DMSO-differentiated cells.

Figs 1→3. Fluorescent labelling in undifferentiated and PMA- and DMSO-differentiated U937 cells. DMSO (1%) induces differentiation to the PMN phenotype, whereas 10 nM PMA induces differentiation to the monocyte/macrophage phenotype.

Figs 1a & b. Fluorescent labelling for cathepsin B.

Undifferentiated U937 cells (Fig. 1a) and cells differentiated with DMSO show weak to negative labelling for cathepsin B (40 µg/ml) (results resembling 1a, not shown), while PMA differentiated (Figure 1b) show polarised labelling for cathepsin B.

Figs 2a & b. Fluorecent labelling for cathepsin D.

Immunolabelling with anti-human cathepsin D serum (1/40) gave relatively strong labelling of undifferentiated (Figure 2a) and PMA-differentiated U937 cells (Figure 2b). No labelling was seen in DMSO-differentiated cells (results not shown).

Figs 3a & b. Fluorescent labelling for the mannose-6-phosphate receptor.

Immunofluorescence labelling shows the presence of M-6-P receptor in PMA-differentiated cells only (Fig. 3b), Fig. 3a illustrates the labelling results seen in the undifferentiated cells. Similar results are seen in DMSO-differentiated cells (results not shown).

Bar scale of all micrographs = 10 µm

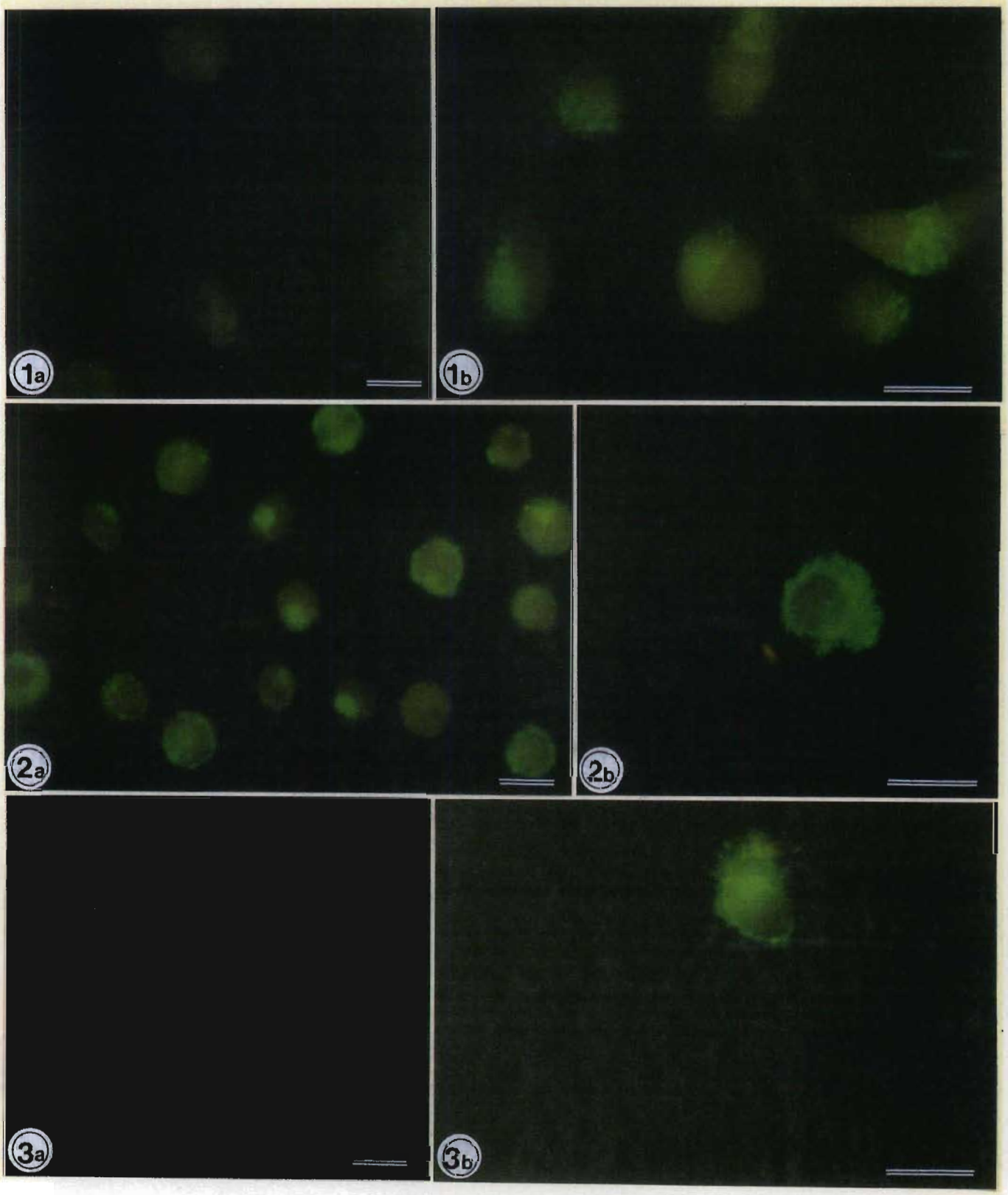
1a
1b
2a
2b
3a
3b

PLATE 16

Confocal and immunofluorescence labelling of permeabilised MCF-10A and Neo-T cells for procathepsin B and cathepsin B, using polyclonal and monoclonal antibodies.

Figs 1→4. MCF-10A and Neo-T cells fluorecently labelled with the anti-ppB22-36 procathepsin B peptide antibody (730 μg/ml) (except Fig. 3a).

Figs 1 & 4. Immunolabelling of a Neo-T cell for procathepsin B.

Fig. 1 is a confocal image, while Fig. 4 is a normal immunofluorescence image. Immunolabelling indicates that organelles containing procathepsin B are spread out away from the nucleus (less perinuclear) than labelling in MCF-10 A cells (Figs 2 and 3b).

Figs 2 & 3a & b. Immunolabelling of an MCF-10 A cell for procathepsin B.

Fig. 2 is a normal epifluorescence image, while Figs 3a and 3b are confocal images. Fig. 3a is the phase image of Fig. 3b, allowing the outer limit of the cell to be seen. Immunolabelling indicates that organelles containing procathepsin B are more perinuclear than those seen in Neo-T cells (Figs 3a and 3b).

Figs 5 & 8. Labelling for cathepsin B using a polyclonal sheep anti-mature human liver cathepsin B antibody.

Confocal images of labelling with the sheep polyclonal antibody (300 μg/ml) gave poor, non-punctate labelling. MCF-10 A cells (Fig. 5) can, however, be seen to have more perinuclear labelling than seen in Neo-T cells (Fig. 8).

Figs 6 & 7. Immunofluorescence labelling using the anti-B192-201 anti-mature cathepsin B peptide antibody.

Conventional immunofluorescence labelling of MCF-10A (Fig. 6) and Neo-T cells (Fig. 7) using the anti-B192-201 peptide antibody (739 μg/ml) gave poor immunolabelling as background labelling is high and some nuclear labelling occured.

Bar scale of all micrographs = 10 μm

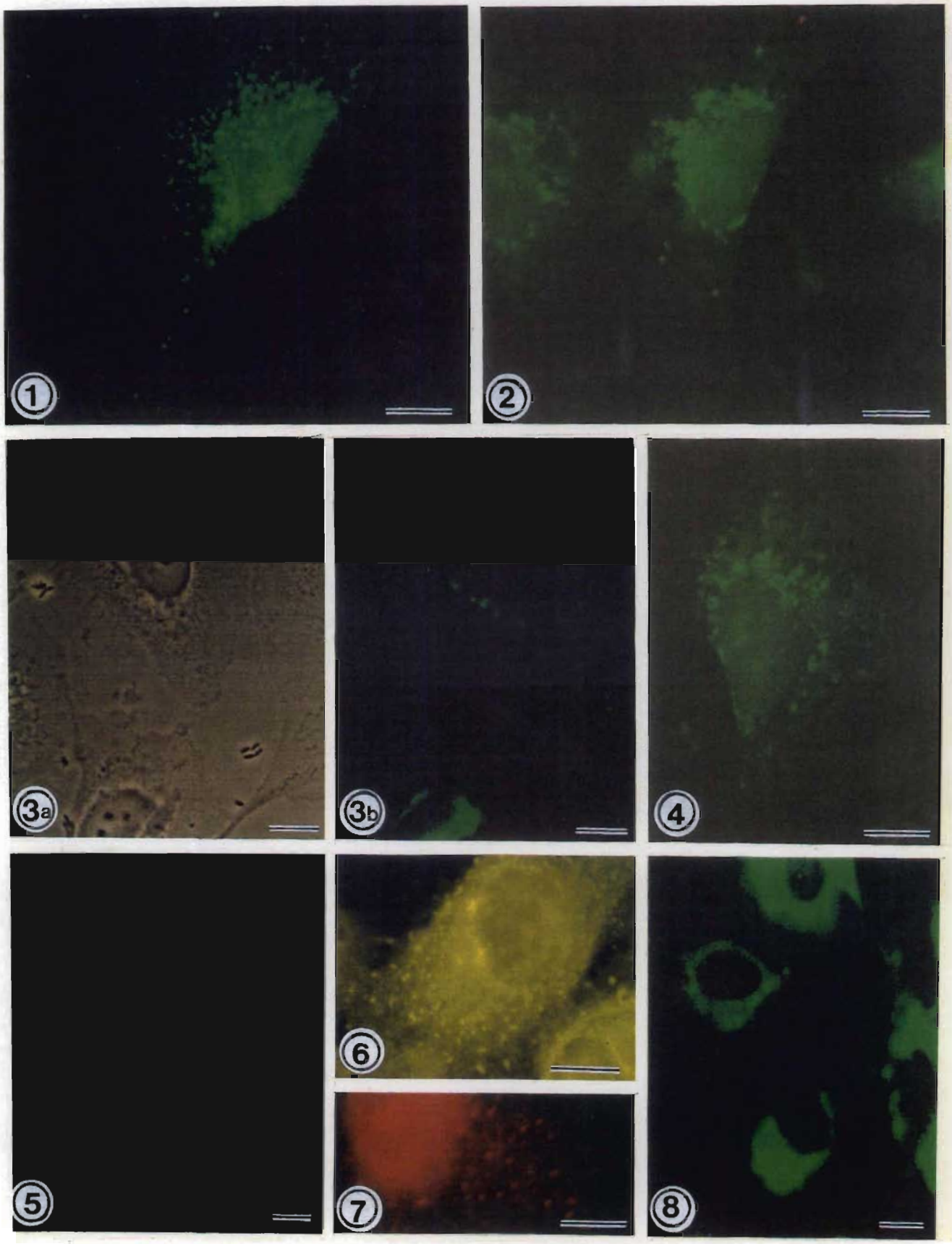
1
2
3a
3b
4
5
6
7
8

PLATE 17

Single and double immunofluorescence labelling of MCF-10A and Neo-T cells for cathepsin D, and cathepsin L.

Figs 1→4. Immunolabelling performed using the chicken anti-porcine cathepsin D antibody (306 µg/ml) and/or the rabbit anti-sheep cathepsin L antibody, detected with the CY3™-labelled, affinity purified, rabbit anti-chicken IgY, not adsorbed against IgGs of other species (used at 1/60) (red fluorecence), or the DTAF-labelled, affinity purified, donkey anti-rabbit conjugate, pre-adsorbed against bovine, goat, horse, human, mouse, rat and sheep IgG, to eliminate cross-reactivity (used at 1/40) (yellow or green labelling).

Figs 1 & 2. Confocal images of fluorescent labelling with the chicken anti-cathepsin D.

Fig. 1 represents immunolabelling of an MCF-10A cell, while Fig. 2 is of a Neo-T cell. Notice the less perinuclear labelling in the Neo-T cell.

Figs 3→4. Double labelling of MCF-10A and Neo-T cells for cathepsins D and L.

Figs 3a and 3b are images of the same MCF-10A cell, labelled for both cathepsin D (Fig. 3a) and cathepsin L (Fig.3b), while Figs 4a and 4b are the equivalent labellings of a Neo-T cell.

Notice that cathepsin D is present in larger quantities than cathepsin L in both cells, that cathepsins D and L colocalise more in the MCF-10A cells (Figures 3a and b) than in the Neo-T cell (Figures 4a and b), and that the distribution of proteinases is slightly less perinuclear in the Neo-T cells (note magnification differences in assessing differences). Background labelling unfortunately arose possibly due to the poorer quality of the CY3-labelled, affinity purified, rabbit anti-chicken antibody.

Bar scale for all micrographs = 10 µm.

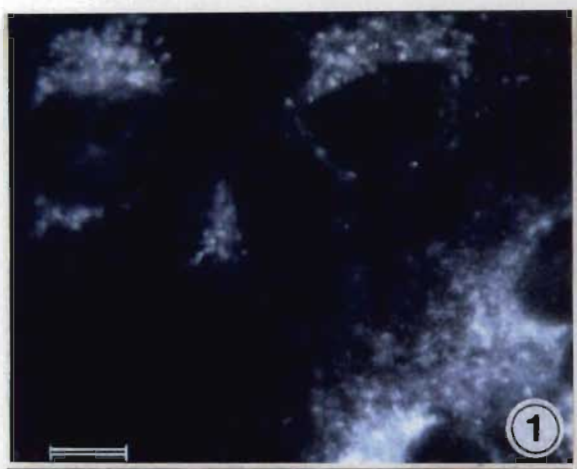

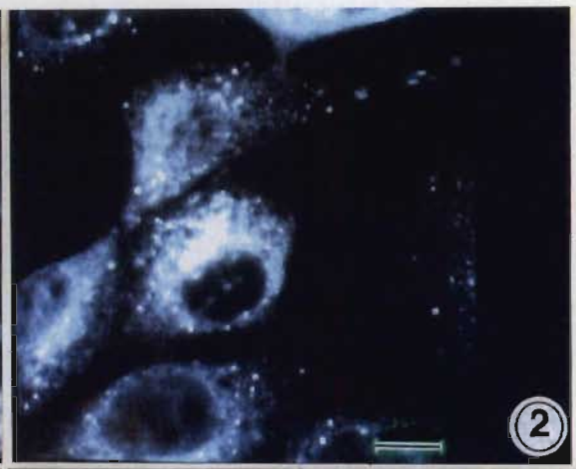

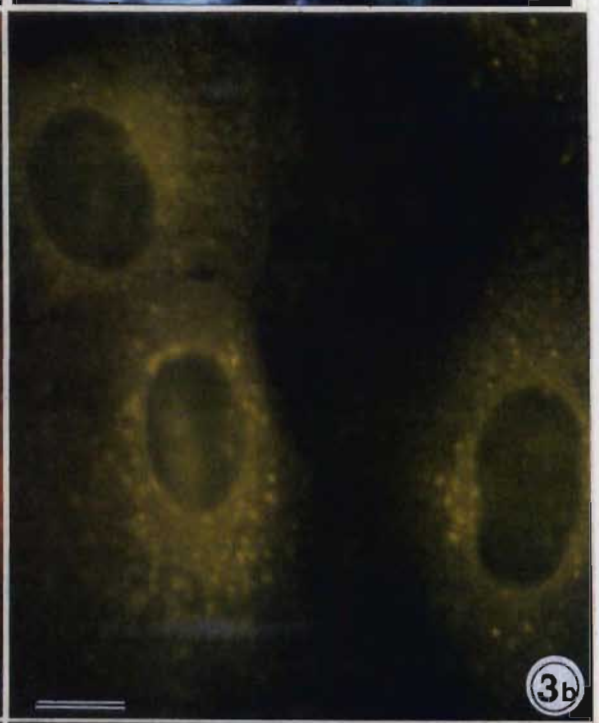

PLATE 18

Immunofluorescence labelling of MCF-10A and Neo-T cells for β tubulin and cathepsin L, using peptide and polyclonal antibodies.

Figs 1→4. Immunofluorescence labelling for β tubulin was performed using a mouse monoclonal antibody (200 μg/ml), detected with a Texas Red-labelled goat anti-mouse conjugate (1/40); for cathepsin L, using the anti-cathepsin L peptide antibody (raised against the sequence equivalent to sequence 1 (Fig. 11, Section 3.3), of cathepsin L, Section 3.3, as chosen for the production of the anti-B192-201 antibody) (394 μg/ml) or the polyclonal rabbit anti-sheep antibody (386μg/ml). Detection of the rabbit antibodies was with a DTAF-labelled, affinity purified, donkey anti-rabbit conjugate (used at 1/40).

Figs 1&2. Double labelling of MCF-10A and Neo-T cells for β tubulin and cathepsin L, using the peptide antibody.

Double immunolabelling of a Neo-T cell (Figs 1a and 1b) and MCF-10A cell (Figs 2a and 2b) for β tubulin (Figs 1a and 2a), and cathepsin L (Figs 1b and 2b), was performed using epifluorescence. Comparison of the images of the Neo-T cell for the two antigens (Figs 1a and 1b) and the images of the MCF-10A cell (Figs 2a and 2b) show that organelles containing cathepsin L are arranged allong microtubule tracks, the microtubule distribution in the Neo-T cell being more extended than that in the MCF-10A cell (compare Figs 1a and 2a), and hence the organelles have a less perinuclear arrangement in the Neo-T cell.

Figs 3 & 4. Labelling of MCF-10A and Neo-T cells for β tubulin and cathepsin L, using the polyclonal antibody.

A similar distribution of immunolabelling as seen with the peptide antibody (Figs 1b and 2b) is seen in labelling of a Neo-T cell (Fig. 3) and an MCF-10A cell (Fig. 4), using the polyclonal rabbit anti-sheep antibody.

Bar scale of all micrographs = 10 μm.

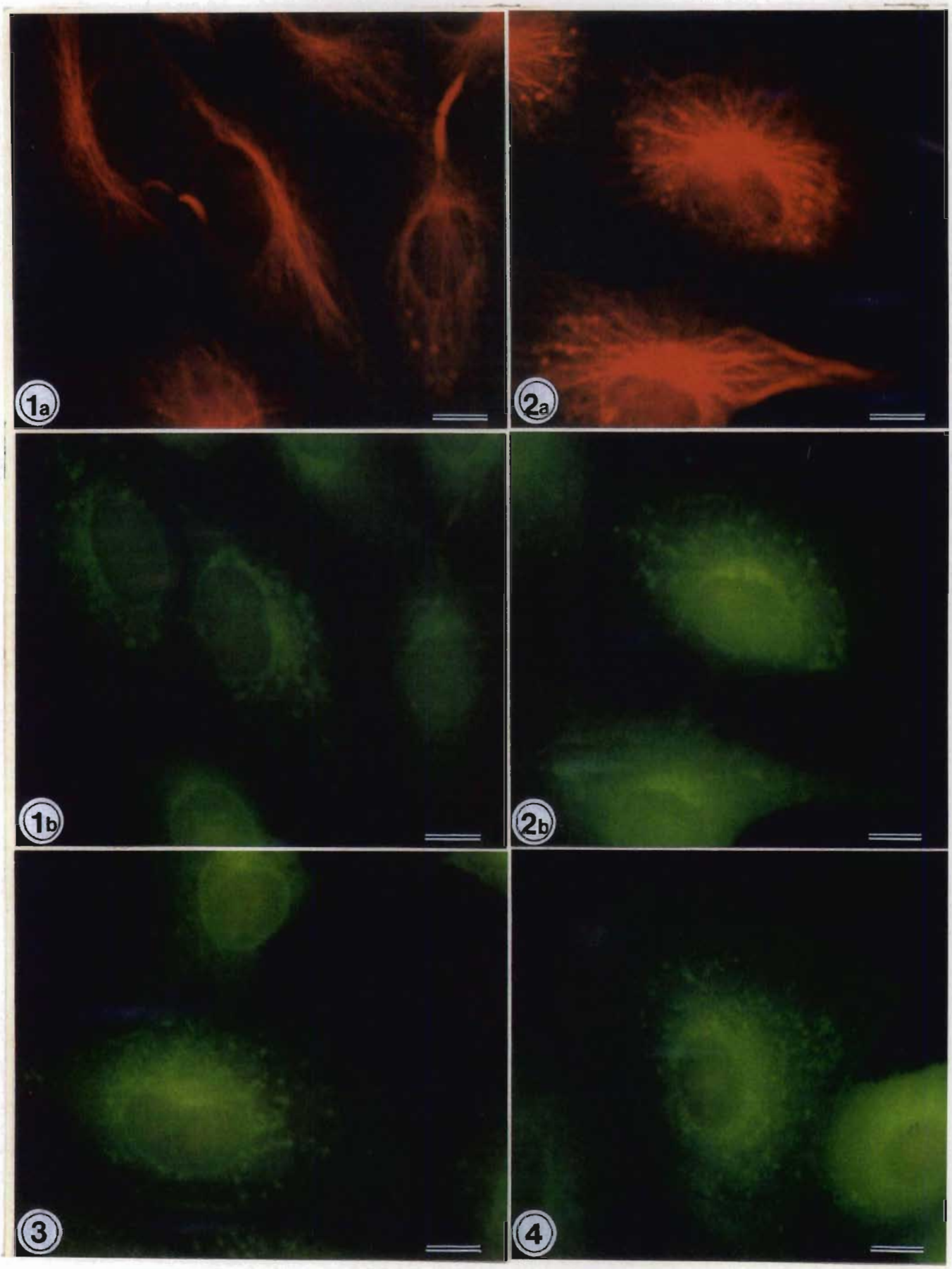
1a
2a
1b
2b
3
4

PLATE 19

Epifluorescence and confocal images of MCF-10A and Neo-T cells labelled with a peptide antibody raised against cathepsin H.

Figs A→F. Immunolabelling for cathepsin H was done using using the anti-cathepsin H peptide antibody [raised against the sequence equivalent to sequence 1 (Figure 11, Section 3.3), of cathepsin H, as chosen for the production of the anti-B192-201 antibody] (412 μg/ml). Detection was with a DTAF-labelled, affinity purified, donkey anti-rabbit conjugate (used at 1/40).

Figs A & B. Epifluorescence images of cells labelled for cathepsin H.

A similar distribution of labelling for cathepsin H is seen in the Neo-T cell (Fig. B), and the MCF-10A cell (Fig. A), using epifluorescence labelling. See, however, confocal images (Figs. C→F).

Figs C→F. Confocal images of cells labelled for cathepsin H.

Images C and D are confocal superimpositions of the phase image on the labelling result, allowing assessment of the distribution of labelling, relative to the cell periphery. These cells were confocally scanned for the plane within the cell giving the greatest labelling intensity. This was found to be the apical surface in the NeoT cell (Figs D and F) and the basolateral surface of the MCF-10A cell (Figs C and E) (focal plane being measured on the "z-scale", a larger number indicating more apical distribution). Notice also that labelling is more spread in the NeoT cell (Fig. F) compared to the MCF-10A cell (Fig. E).

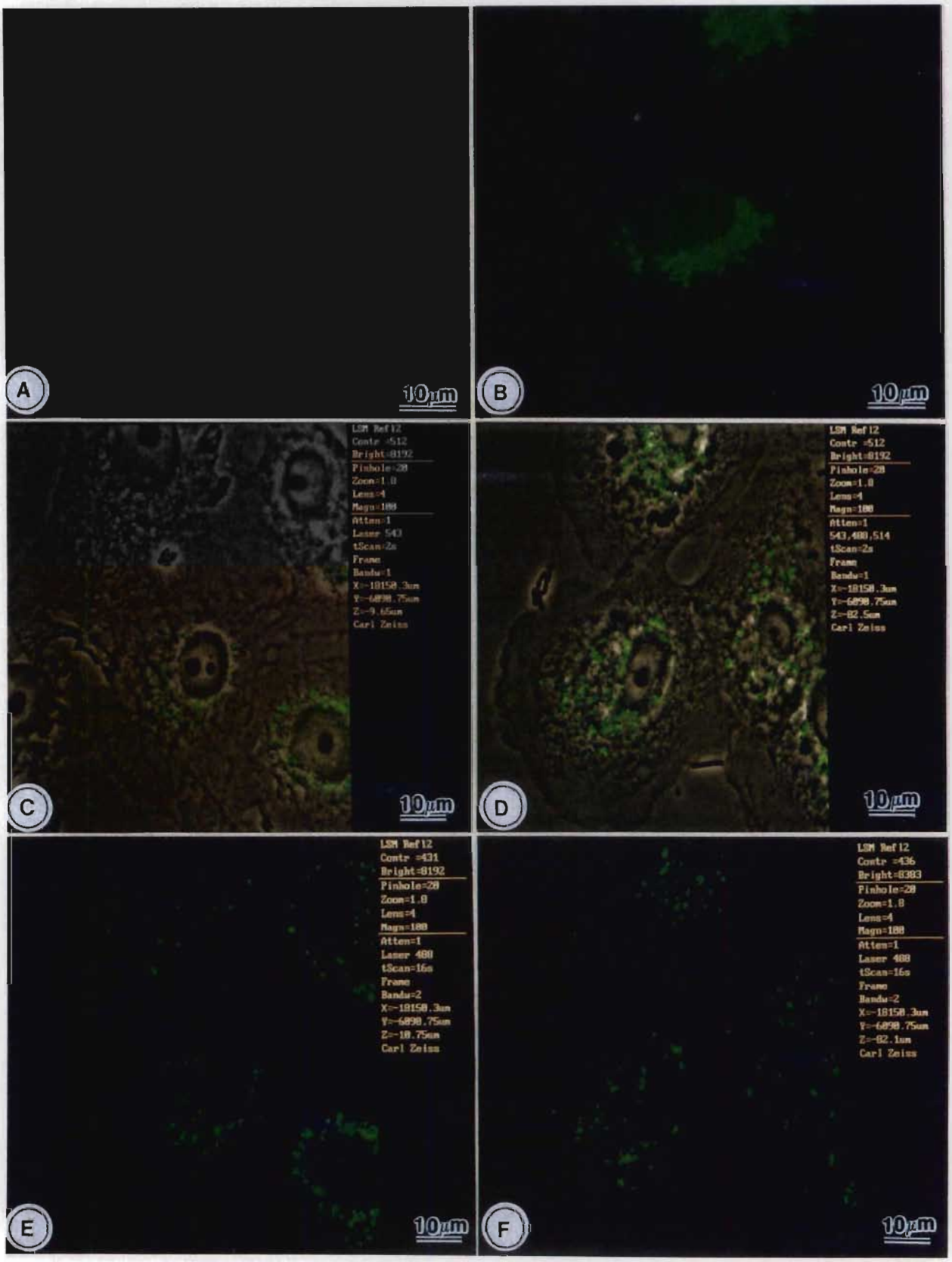
A
10µm
B
10µm
LSM Ref12
Contr =512
Bright=8192
Pinhole=28
Zoom=1.0
Lens=4
Magn=100
Atten=1
Laser 543
tScan=2s
Frame
Bandw=1
X=-18150.3um
Y=-6898.75um
Z=-9.65um
Carl Zeiss
C
10µm
LSM Ref12
Contr =512
Bright=8192
Pinhole=28
Zoom=1.0
Lens=4
Magn=100
Atten=1
543,480,514
tScan=2s
Frame
Bandw=1
X=-18150.3um
Y=-6898.75um
Z=-82.5um
Carl Zeiss
D
10µm
LSM Ref12
Contr =431
Bright=8192
Pinhole=28
Zoom=1.0
Lens=4
Magn=100
Atten=1
Laser 488
tScan=16s
Frame
Bandw=2
X=-18150.3um
Y=-6898.75um
Z=-10.75um
Carl Zeiss
E
10µm
LSM Ref12
Contr =436
Bright=8383
Pinhole=28
Zoom=1.0
Lens=4
Magn=100
Atten=1
Laser 488
tScan=16s
Frame
Bandw=2
X=-18150.3um
Y=-6898.75um
Z=-82.1um
Carl Zeiss
F
10µm

PLATE 20

Confocal and epifluorescence images of MCF-10A and Neo-T cells labelled for the mannose-6-phosphate receptor.

Figs 1&2. Confocal images of MCF-10A and Neo-T cells labelled for the M-6-P receptor.

Figs 1a, b and c are images of an MCF-10A cell labelled for the M-6-P receptor (antiserum diluted 1/20). Figs 1a and 1b have labelling superimposed on the phase image and show an extensive tubular network, of possible lysosomal origin, in a cell (lower right hand corner) (See Chapter 6), and moderate numbers of M-6-P receptor. Comparable labelling images of the Neo-T cells show fewer M-6-P receptors (Fig. 2).

Figure 3. Epifluorescence image of a Neo-T cell labelled for the M-6-P receptor.

Epifluorescence image of a Neo-T cell shows similar low levels of receptor compared to that seen in the MCF-10A equivalent.

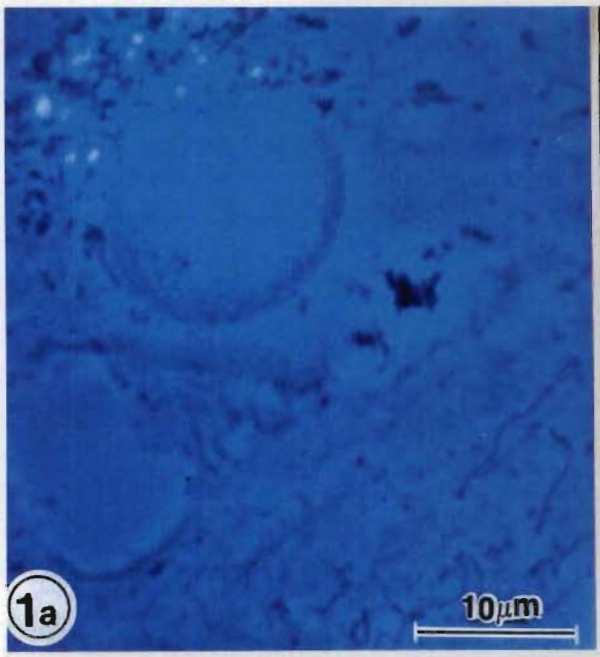
1a
10μm


1b
10μm

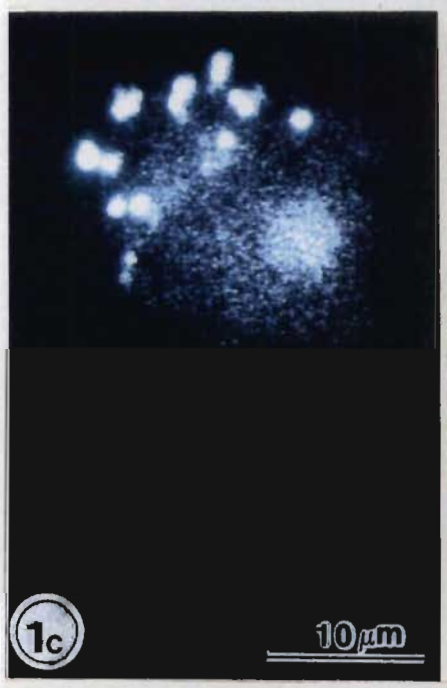
1c
10μm

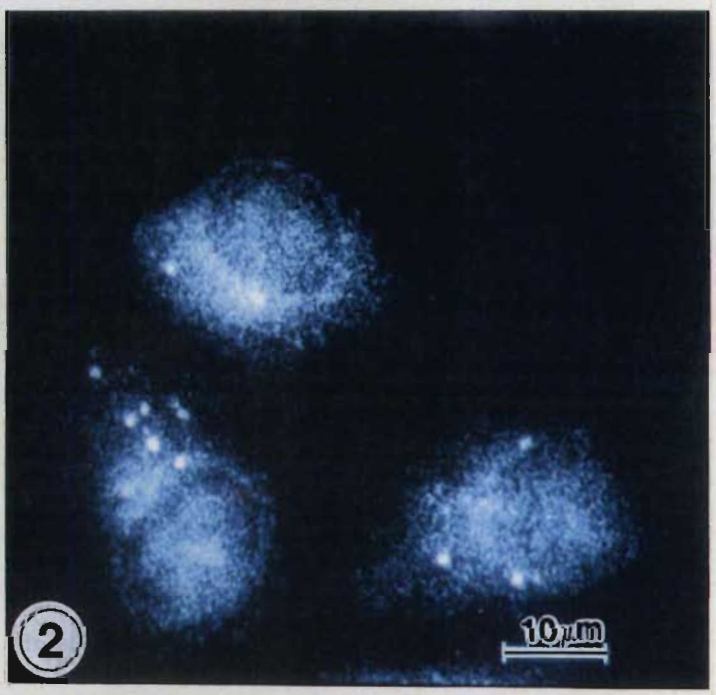
2
10μm

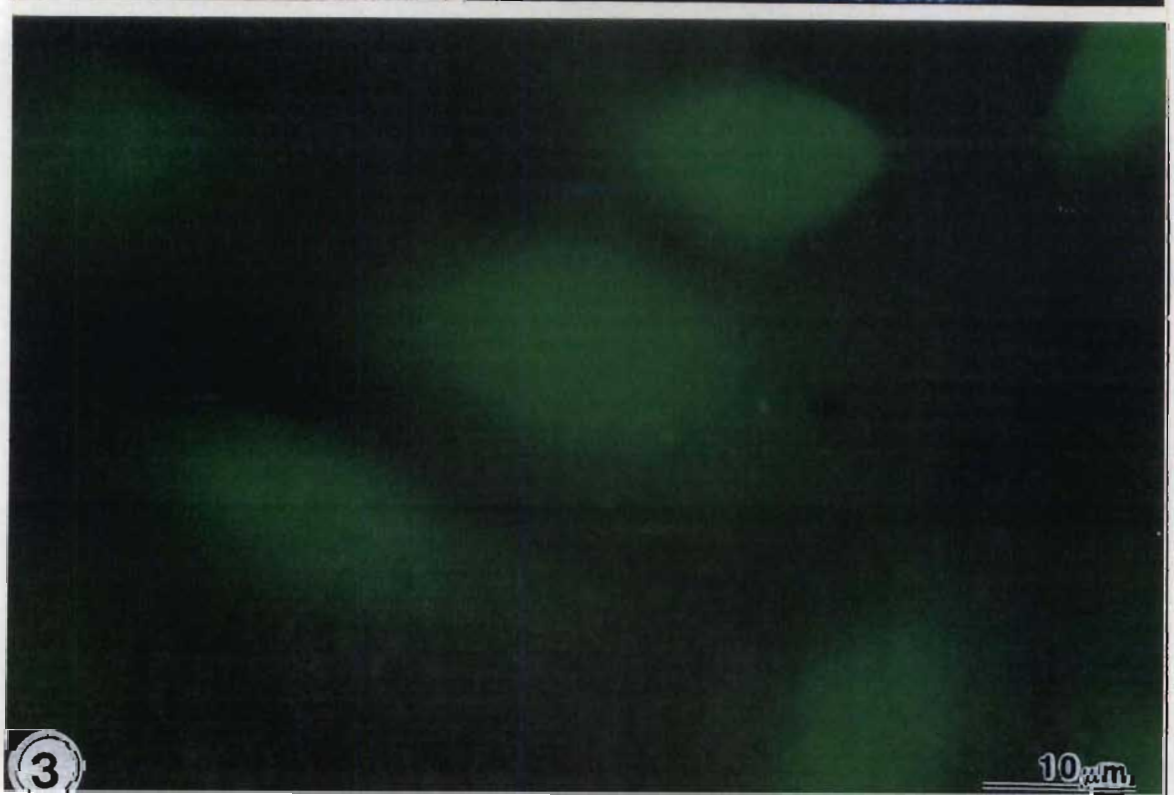
3
10μm

PLATE 21

Lowicryl sections of MCF-10A and Neo-T cells, sectioned perpendicular to the basal surface of the cell.

Figure 1. Neo-T cells showing possible aberrant vesicle formation.

Two cells [indicated by presence of two nuclei (N) sectioned vertically (basal surface being indicated with arrowheads)], show vesicle formation over the entire length of the cell (arrows). Neo-T cells seem to contain more vesicles than the MCF-10A cells cultured under similar conditions (see Fig. 2). Note that both cells are non-adherent, a possible reason for the observed morphology, may be the development of the MCF-F phenotype (see Section 5.4.3).

Figure 2. MCF-10A cell showing more vesicle formation in non-adherent than adherent cells.

A vertical resin section shows three cells (lower, upper cell, and middle cell indicated with large arrows, basal surface indicated with arrowheads). The non-adherent and semi-adherent cell in the middle shows a greater number of electron-translucent vesicles and "autophagic vacuoles" than adherent cells. A greater number of tonofilaments (electron-dense filaments that are normal components of the MCF-10 cells) are evident.

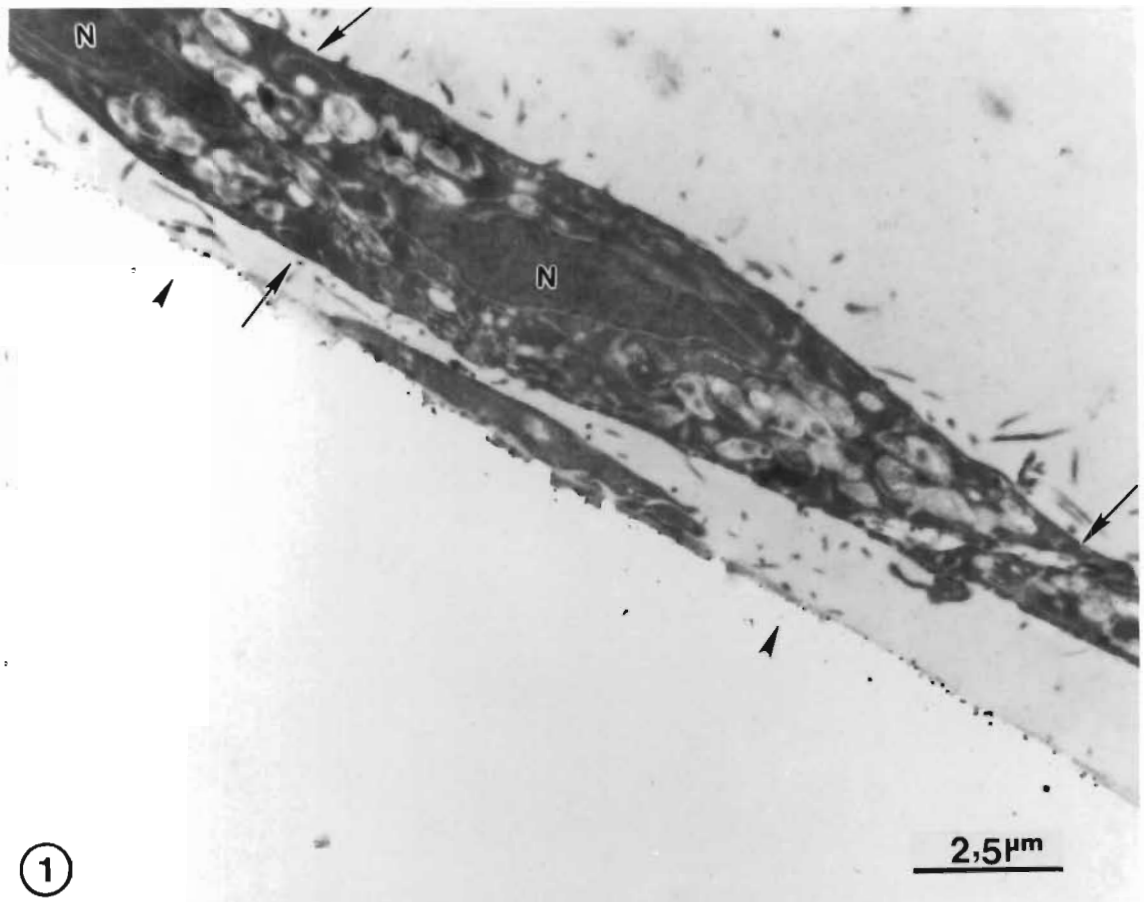

①

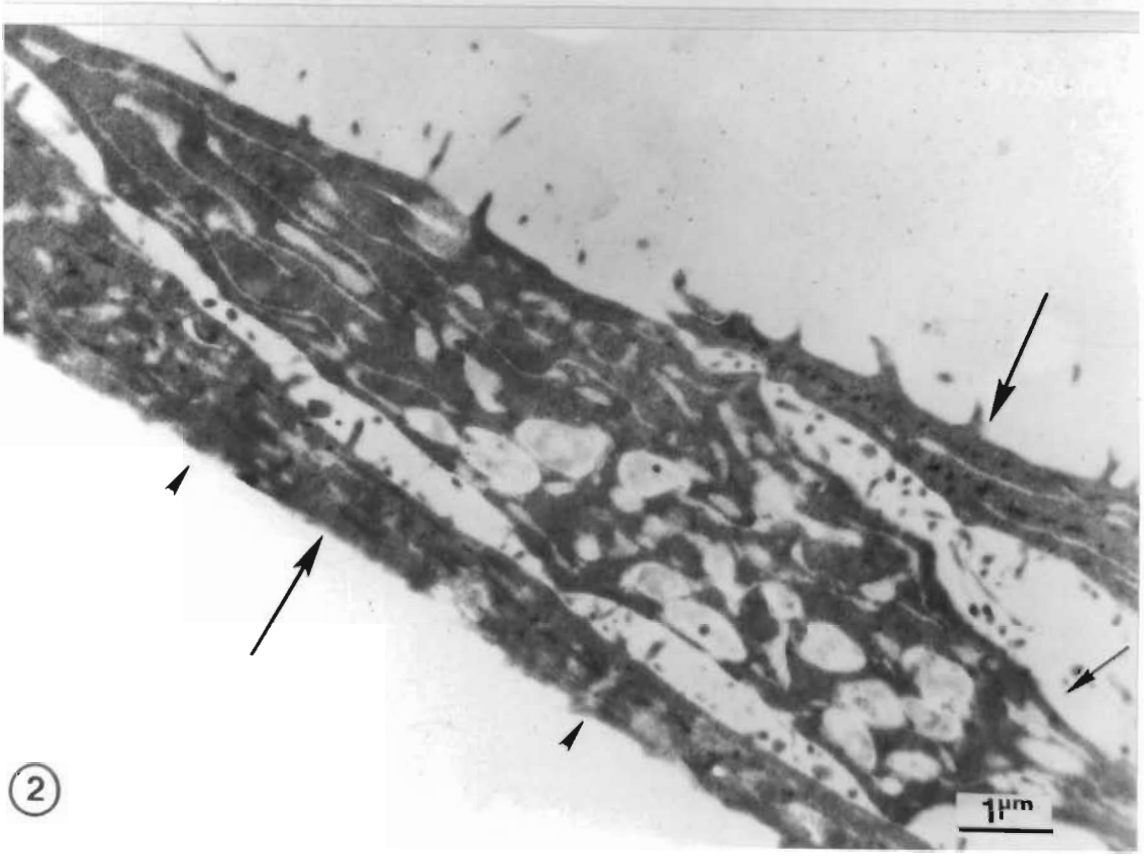

②

PLATE 22

Vertical section of Neo-T cells embedded in Lowicryl resin, showing large autophagic vacuole and other vesicles.

Figure 1. Neo-T cells showing "adherent" and "non-adherent" morphology.

The cell on the right is adherent (arrowheads indicating the basal surface), and shows fewer vacuoles (large arrows indicating vacuoles in both cells).
N= nucleus.

Figure 2. Enlarged view of non-adherent Neo-T cell showing "autophagic vacuole".

Neo-T cell shows central "autophagic vacuole" or secretory vesicle (Section 5.4.3) containing electron-dense material (large arrow). Cells contain numerous mitochondria (m or arrowheads), Golgi systems (G) and numerous microvilli extend off the external membrane.

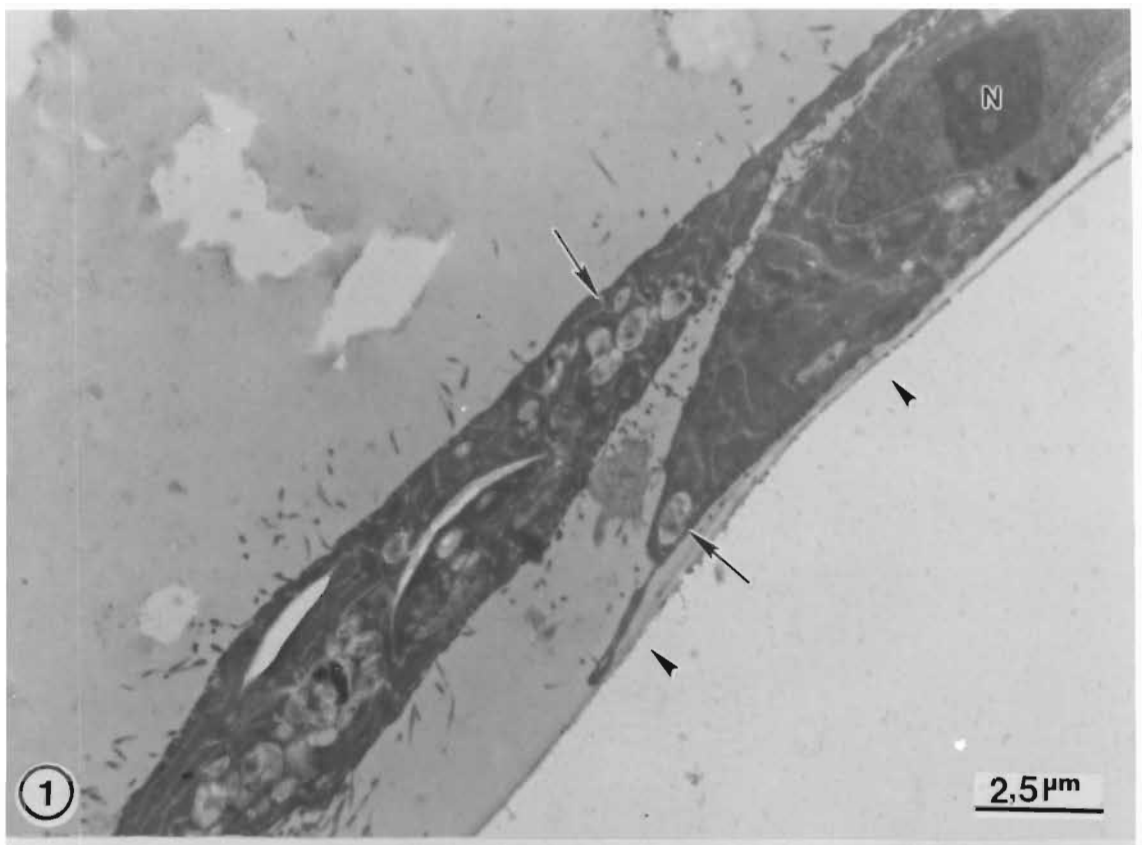

1

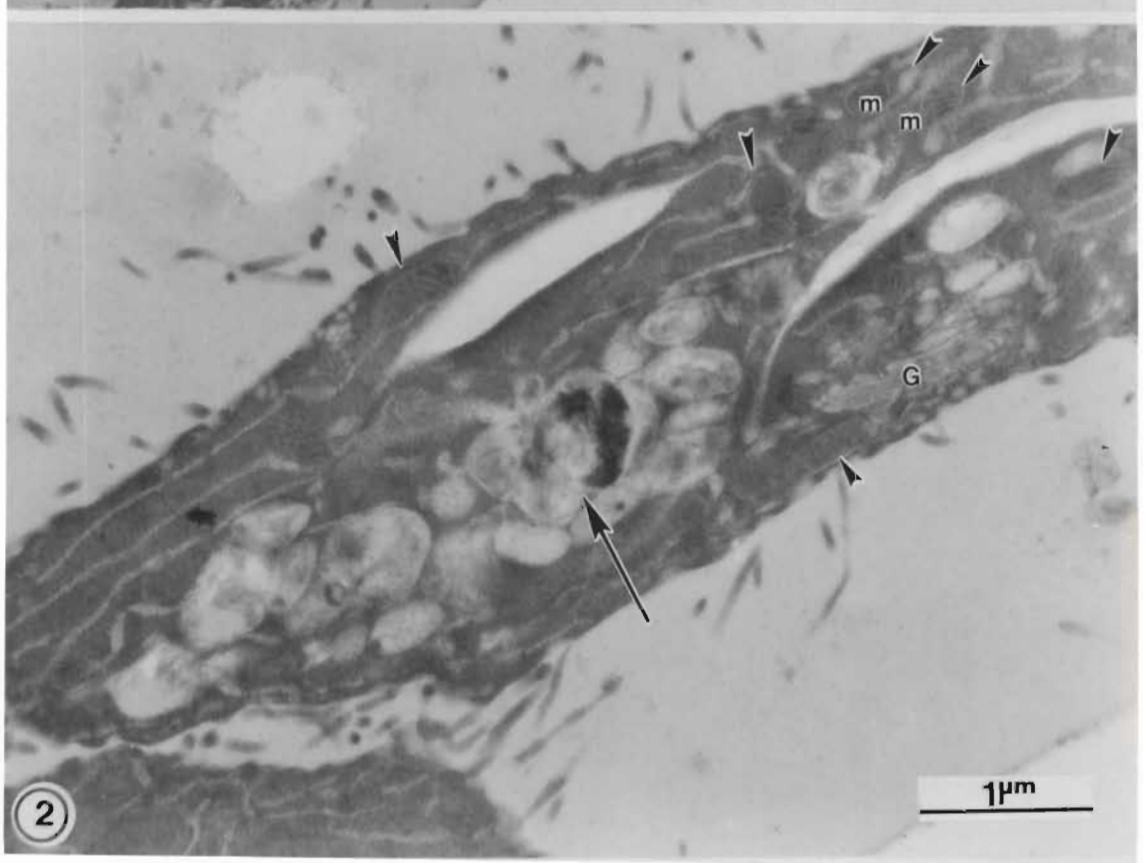

2

PLATE 23

Lowicryl sections showing detail of "autophagic" vacuoles in Neo-T cells, and their content of cathepsins D and B .

Figure 1. Detail of electron-translucent "autophagic vacuole" showing labelling for cathepsin B.

Immunolabelling was performed with sheep anti-human liver cathepsin B antibody (0.2 µg in 10 µl), followed by rabbit anti-sheep antibody and a 5 nm protein A gold label.
"Autophagic" or secretory vacuoles appear as a complicated conglomerate of membrane-bound, electron-translucent, swollen vesicles, all of which are seen here to label for cathepsin B (arrowheads). Some cathepsin B seems also to be secreted between cells (arrow). Similar organelles were seen to occur in MCF-10A cells.

Figure 2. Detail of "electron-dense" autophagic vacuole and cathepsin D immunolabelling.

Immunolabelling was performed with chicken anti-porcine D antibody (2.5 µg in 10 µl) and labelling detected with a 5 nm protein A gold probe. A similar complicated aggregation of organelles are seen around the electron-dense product or autocatalysed material (large arrow). Cathepsin D occurs in almost all surrounding vesicles (arrowheads), but only very little is associated with the electron-dense material.

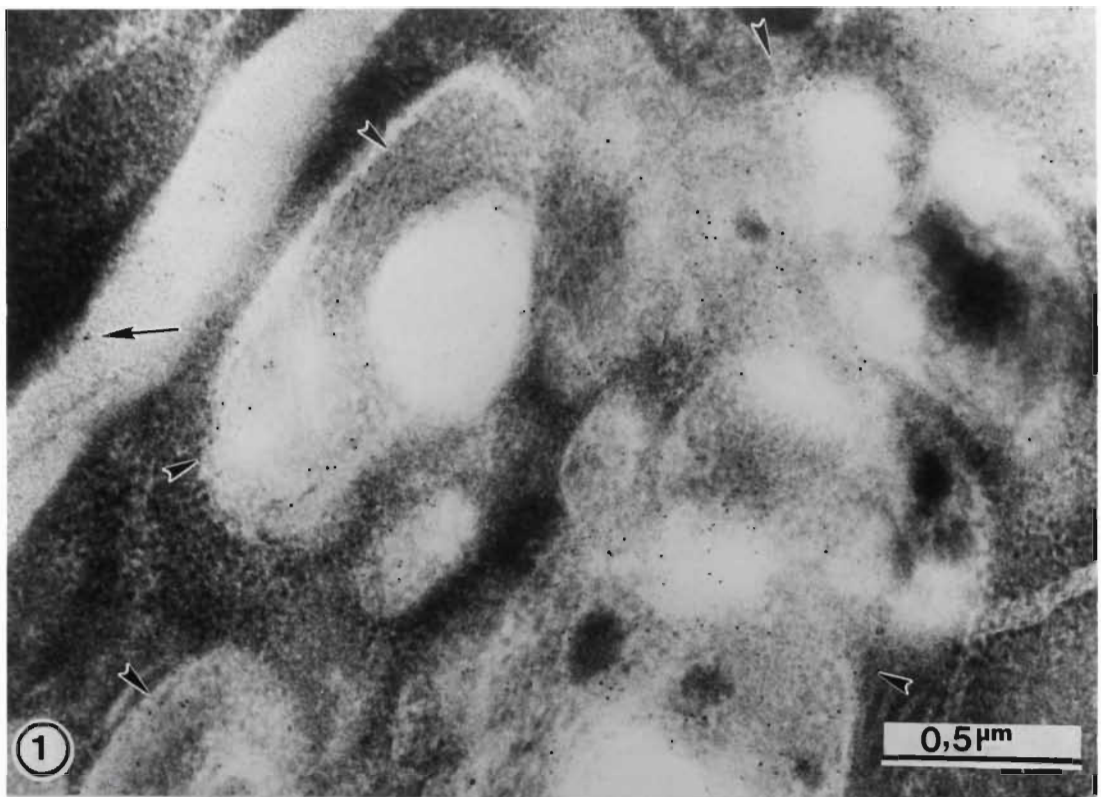

1

2

PLATE 24

Lowicryl section of "autophagic vacuoles" in MCF-10A and Neo-T cells, double labelled for cathepsins B and D.

Figs 1 & 2. Double labellings were performed with the chicken anti-porcine cathepsin D antibody (2.5 μg in 10 μl), followed by rabbit anti-chicken antibody and a protein A gold probe (5 nm), and with the sheep anti-human liver cathepsin B antibody (0.2 μg in 10 μl) followed by rabbit anti-sheep antibody and a larger protein A gold probe (10 nm).

Figure 1. "Autophagic vacuole" and electron-translucent vesicles in a Neo-T cell, double labelled for cathepsin D and cathepsin B.

Small arrows indicate vesicles containing both cathepsin D (5 nm particle) and cathepsin B (10 nm particle). The large arrow, indicates a vesicle containing only cathepsin D, and the small arrowhead indicates vesicles apparently containing no cathepsins B or D.

Figure 2. Detail of an MCF-10A cell with double labelling of "autophagic vacuole" for cathepsins D and B.

Small arrow indicates vesicle containing both cathepsin D (5 nm particle). and cathepsin B (15 nm particle). Large arrow indicates vesicle containing only cathepsin D. Notice how enzymes appear to associate into aggregates.

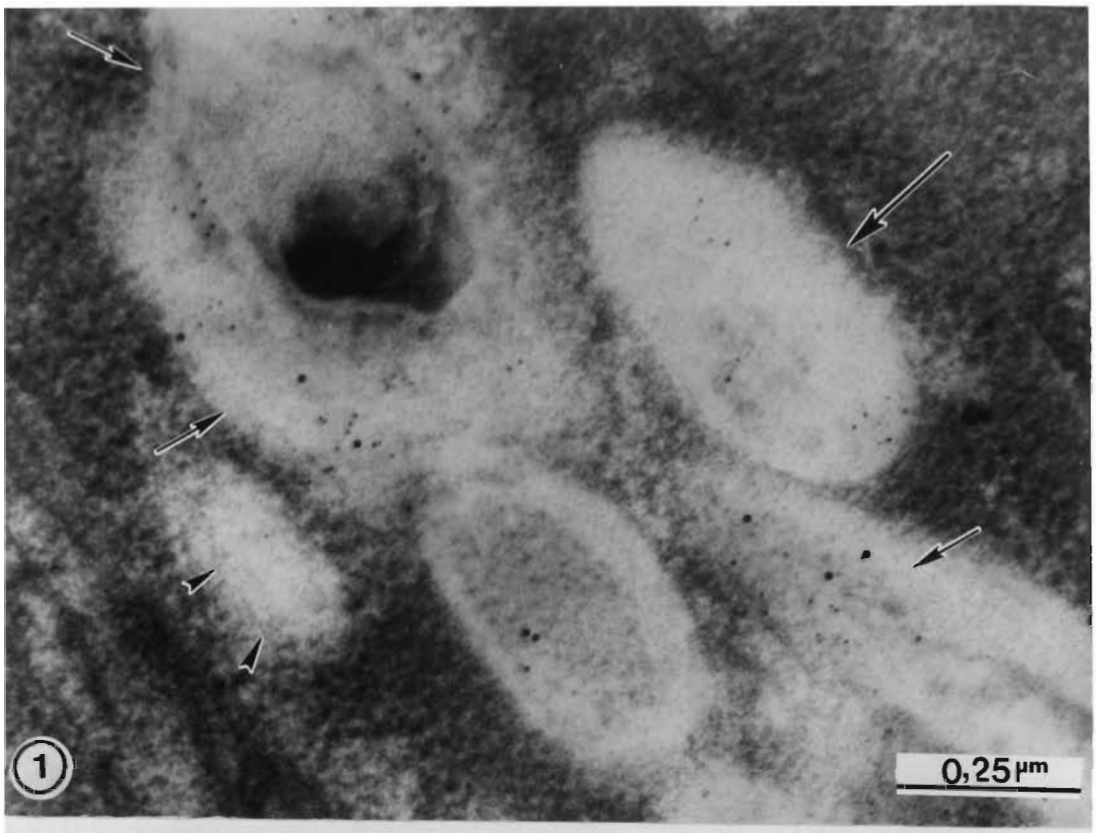
1
0,25 µm


2
0,1µm

PLATE 25

Lowicryl section of a Neo-T cell showing association of cathepsin B with the microvilli and vesicles in cell protruberances.

Figs.1 & 2. Section showing two adjacent Neo-T cells labelled for cathepsin B.

Sections were labelled with sheep anti-human liver cathepsin B antibody (0.2 µg in 10 µl) followed by rabbit anti-sheep antibody and a protein A gold probe (5 nm). Section shows labelling for cathepsin B in a semi-electron-translucent body in one cell (arrowheads above the mitochondria, M) and association of cathepsin B with the external surface of "extensions" or pseudopodia, containing vesicles labelling for cathepsin B, in an adjacent cell (arrowheads).

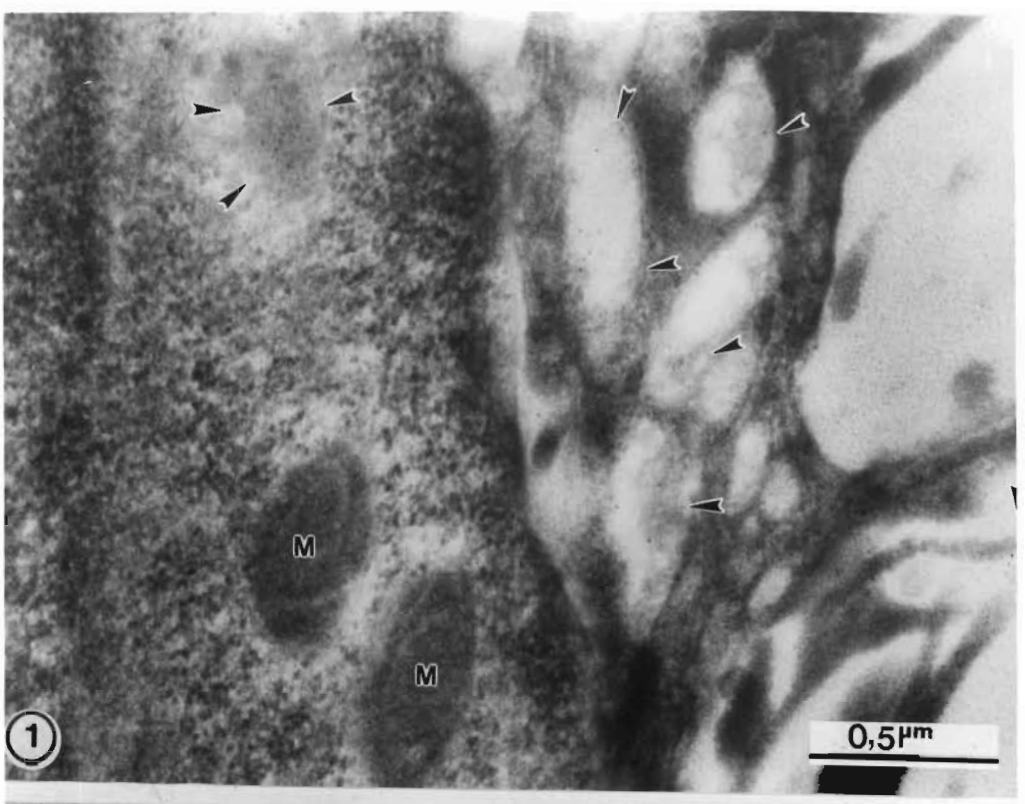

1

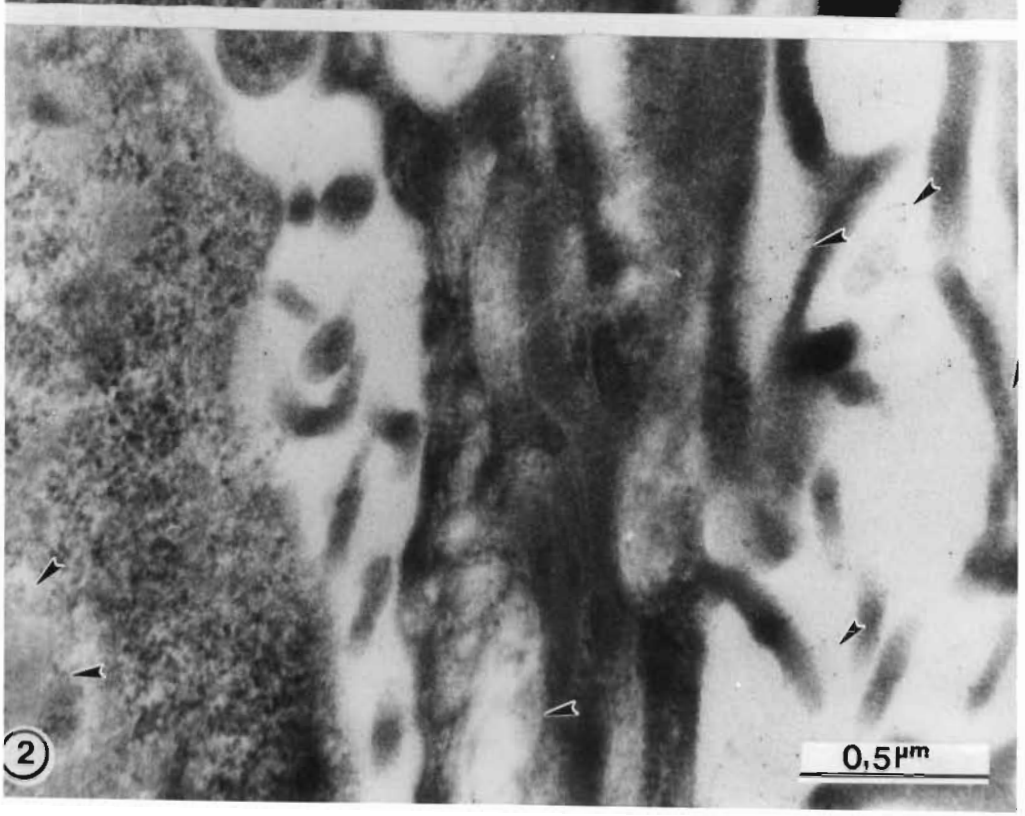

2